Self-assembly of Cuprous Iodide Cluster-based Calix[4]resorcinarenes and Photocatalysis Properties

Chu-Xing Hu[a], Ya-Hui Xuan[a], Zi-Hao Jiang[a], Tao Lu[a], Jie Yang[a], Hui Yuan[a], You-Ping Tian[b]*, Zheng-Guang Sun[a]*, Xuan-Feng Jiang[a]*

[a]Key Laboratory of Green Preparation and Application for Functional Materials, Ministry of Education, Hubei Key Laboratory of Polymer Science, School of Materials Science and Engineering, Hubei University, Wuhan, Hubei, 430062, P. R. China

[b]College of Pharmacy, Guizhou University of Traditional Chinese Medicine, Guiyang, Guizhou, 550025, P.R. China

Table of Contents

S1. General Information

All reagents and solvents were purchased from Macklin Biochemical and Innochem Chemical, and used without further purification. NMR spectra were recorded on either a Bruker AVIII 400 MHz spectrometer or a Bruker AVIII 125 MHz spectrometer and referenced to residual solvent peaks. The working frequencies are 400 for ^{1}H and 125 MHz for ^{13}C. High-resolution mass spectroscopies were collected on ESI-MS and MALDI-TOF-MS spectrometers. FT-IR spectra was collected on a Thermo Nicolet FTIR-IS50 spectrometer. The UV-Vis absorption spectral analyses were carried out on a UV-3600 spectrometer. The Fluorescence spectral analyses were carried out on an Edinburgh FLS980 spectrometer. Single crystal diffraction data of MOF **1** and Cluster **2** was collected on a Bruker D8 Venture APEX II CCD single crystal diffractometer.

S2. Synthesis and characterization of ligands and complexes
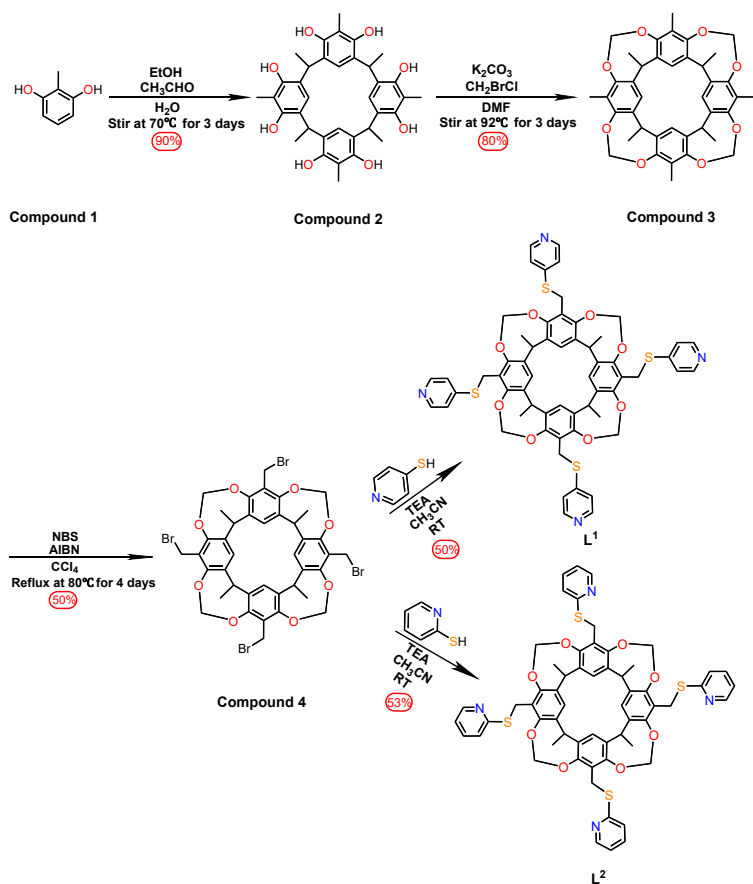
Scheme S1. Synthetic routes of **L¹** and **L²**.

Compound **1** was purchased from commercial regent company (J&K). Compounds **2-4** are synthesized using the similar method reported in previous work.

Add 2,6-dihydroxytoluene (10.28g, 82.8mmol), ethanol (50ml), and acetaldehyde (4.5ml) in a round-bottomed flask in an ice-water bath. The process is carried out under the protection of N_2, and then 36% concentrated hydrochloric acid (30ml) is added dropwise to it. After the addition of hydrochloric acid was completed, the ice-water bath was removed and the reaction was gradually heated to 65°C for 5 hours. Next, the filtrate was obtained by suction filtration, washed with water until the pH was neutral, spin-dried and recrystallized with ethanol to obtain Compound **2** in a yield of 90%. ¹H NMR (400 MHz, DMSO-d_6) δ 8.68 (s, 1H), 7.38 (s, 1H), 4.44 (q, J = 7.2 Hz, 1H), 1.94 (s, 1H), 1.70 (d, J = 7.2 Hz, 1H).

The synthesis of compound **3**. Add compound **2** (3g, 4.62mmol) and potassium

carbonate 7g into a 100ml sealed tube, then 40ml DMF and 7ml chlorobromomethane was poured into above mixture and stirred at 100 °C under N_2 atmosphere for three days. After the reaction, the potassium carbonate was washed with a large amount of water (300 ml) and filtered by suction. The red precipitate was dried under vacuum, followed by purification through chromatographic silica gel column using dichloromethane as the eluent, and then compound **3** was obtained in a yield of 80%. ^{1}H NMR (400 MHz, Chloroform-*d*) δ 7.11 (s, 1H), 5.90 (*d, J* = 6.9 Hz, 1H), 4.99 (*q, J* = 7.3 Hz, 1H), 4.27 (*d, J* = 6.9 Hz, 1H), 1.98 (s, 3H), 1.74 (*d, J* = 7.4 Hz, 3H).

The synthesis of compound **4**. Add compound **3** (1g, 1.54mmol), NBS (1.39g, 7.8mmol), AIBN (0.135g,0.82mmol) to a 100ml round bottom flask, and then carbon tetrachloride (30ml) was added and refluxed at 80°C, during which TLC is used to determine if the reaction is complete. If the reactants are not disappeared, add the same amount of AIBN until the reaction is complete. The reaction was stopped and cooled to room temperature, the crude product was filtered with suction, the solvent was evaporated under reduce pressure and dissolved in dichloromethane, followed by extraction with 1M ($Na_2S_2O_3$/NaOH=1:1) solution to obtain an organic layer. The organic layer was spin-dried, and then hexane/dichloromethane (V: V, 1:5) as a mixed eluent to separate and purify the sample through a chromatographic column. Compound **4** was obtained in a yield of 50% after freeze-drying [1]. ^{1}H NMR (400 MHz, Chloroform-*d*) δ 7.28 (s, 1H), 6.05 (*d, J* = 6.9 Hz, 1H), 5.03 (*q, J* = 7.3 Hz, 1H), 4.59 (*d, J* = 7.3 Hz, 1H), 4.43 (s, 2H), 1.77 (*d, J* = 7.4 Hz, 3H).
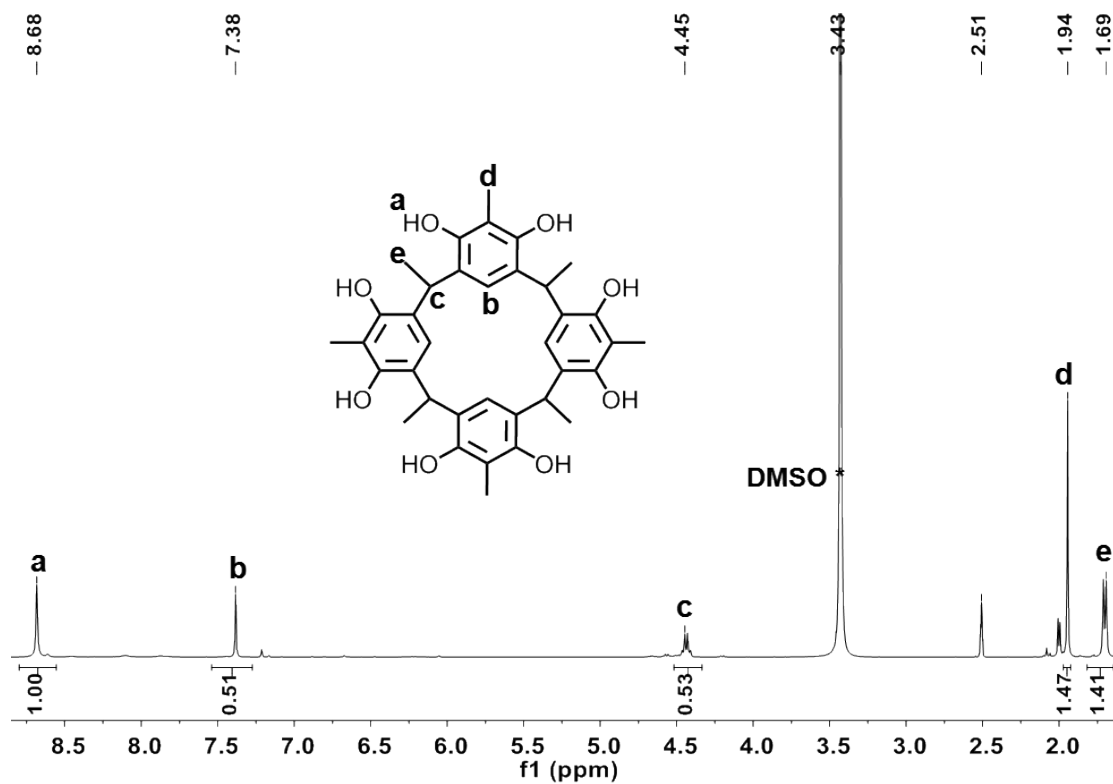
Figure S1. ^{1}H NMR spectrum (298 K, 400 MHz, DMSO-d_6) of compound **2**.
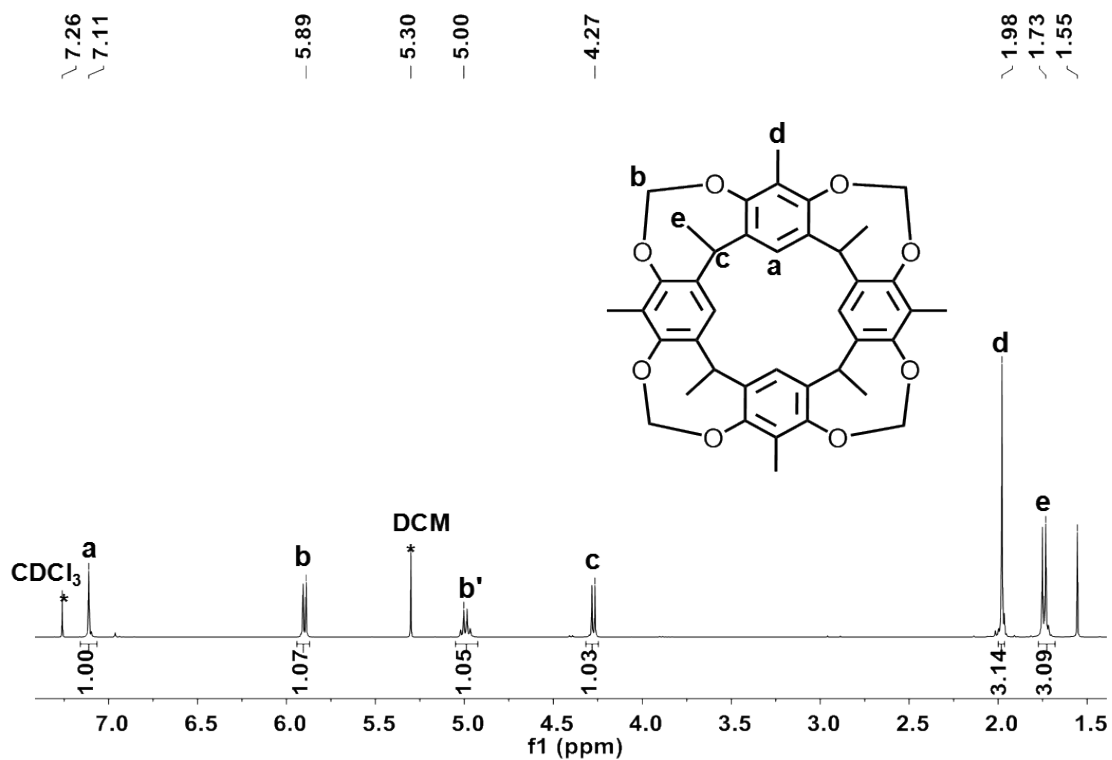
Figure S2. ^{1}H NMR spectrum (298 K, 400 MHz, DMSO-d_6) of compound **3**.
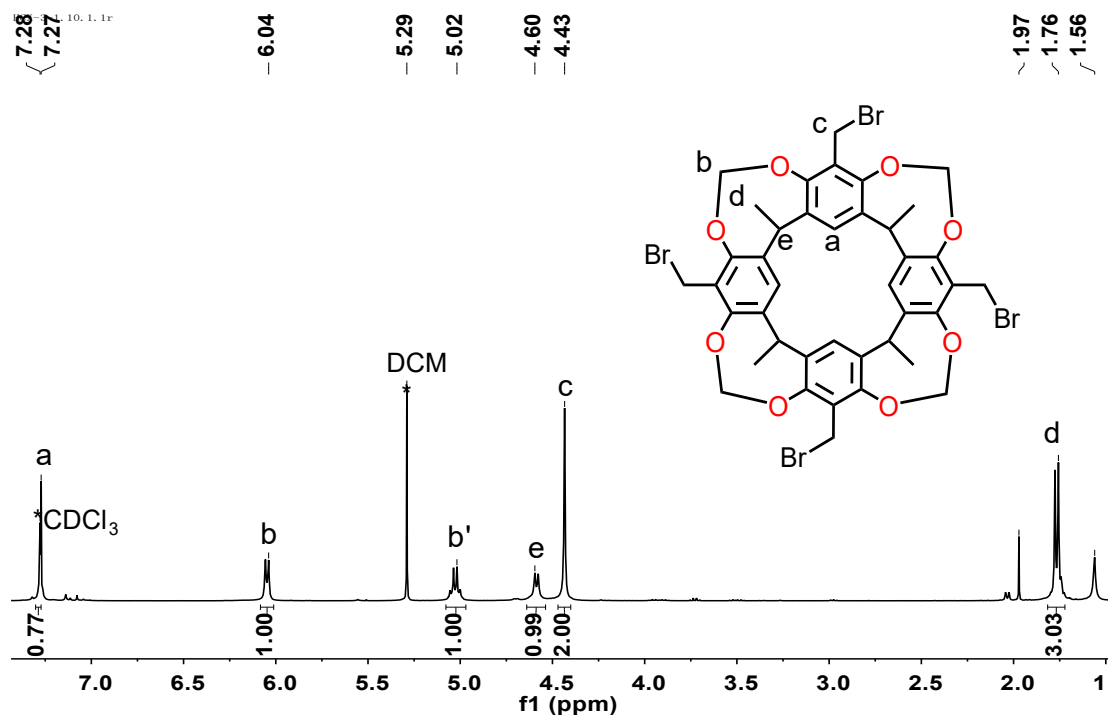
Figure S3. ^{1}H NMR spectrum (298 K, 400 MHz, DMSO-d_6) of compound **4**.

The synthesis of calix[4]resorcinarene ligands **L^1-L^2**.

Compound **4** (418 mg, 0.43mmol) and 4-Mercaptopyridine (208 mg, 1.87mmol) were added in acetonitrile (10 mL) and stirred at 40°C. Triethylamine (0.56 ml, 28.6mmol) was added by syringe and the mixture was stirred for two days. The resulting pale-yellow precipitate was filtered off, washed with water, acetonitrile and dried to afford the desired product as white solid (233.3 mg, 0.22 mmol) in 50% yield. ^{1}H NMR (400 MHz, DMSO-d_6, 298 K, ppm)：^{1}H NMR (400 MHz, DMSO) δ 8.38 (*d*, *J* = 6.2 Hz, 8H), 7.77 (s, 4H), 7.31 (*d*, *J* = 6.3 Hz, 9H), 5.96 (*d*, *J* = 7.7 Hz, 5H), 4.81 (*q*, *J* = 7.0 Hz, 4H), 4.42 (*d*, *J* = 7.7 Hz, 4H), 4.08 (s, 8H), 1.83 (*d*, *J* = 7.4 Hz, 13H).^{13}C NMR (125 MHz, DMSO-d_6) δ158.31, 152.83, 149.79, 139.45, 137.15, 124.18, 122.00, 121.19, 120.41, 99.97, 31.81, 23.66, 16.57. EMS-MS (MeCN, m/z)：[**L^1**+H]$^+$, calcd for $C_{60}H_{53}N_4O_8S_4$ m/z=1085.27 found, m/z=1085.6; [**L^1**+H$_2$O+H]$^+$, calcd for $C_{60}H_{55}N_4O_9S_4$, m/z=1103.3, found, m/z=1103.1; [**L^1**+CH$_3$OH+H]$^+$, calcd for $C_{61}H_{57}N_4O_9S_4^+$, m/z=1117.3, found, m/z=1116.8; [**L^1**+C$_2$H$_5$OH+H]$^+$, calcd for $C_{62}H_{59}N_4O_9S_4^+$, m/z=1131.3, found, m/z=1131.5; [**L^1**+3H$_2$O+CH$_3$OH+H]$^+$,calcd for

$C_{61}H_{63}N_4O_{12}S_4{}^+$, m/z=1171.3, found, m/z=1170.5; $[\mathbf{L^1}+2CH_3OH+K]^+$,calcd for $C_{62}H_{60}N_4O_{10}S_4K^+$, m/z=1187.3, found, m/z=1187.4.
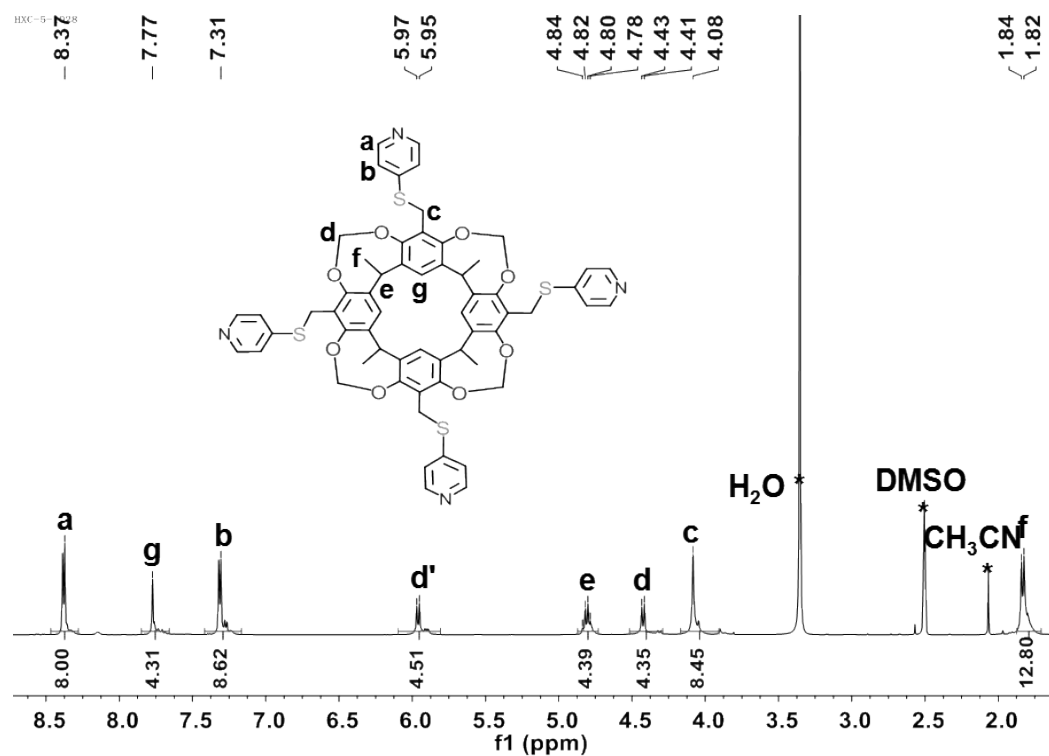
Figure S4. ^1H NMR spectrum (298 K, 400 MHz, DMSO-d_6) of $\mathbf{L^1}$.
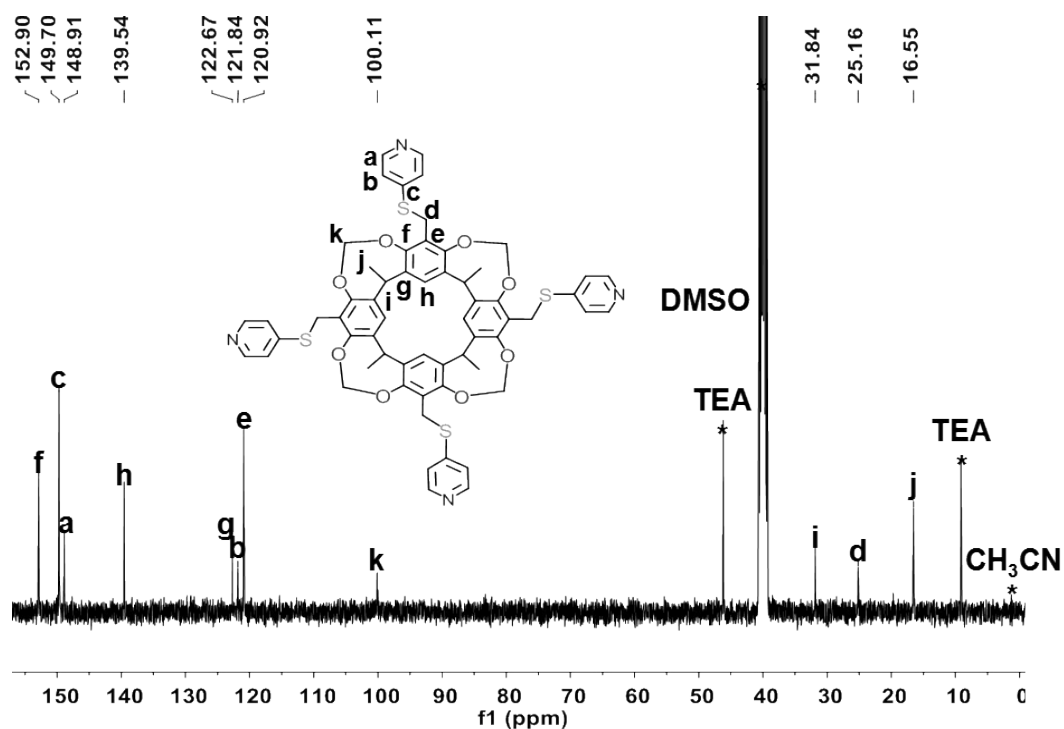
Figure S5. ^{13}C NMR spectrum (298 K, 100 MHz, DMSO-d_6) of $\mathbf{L^1}$.
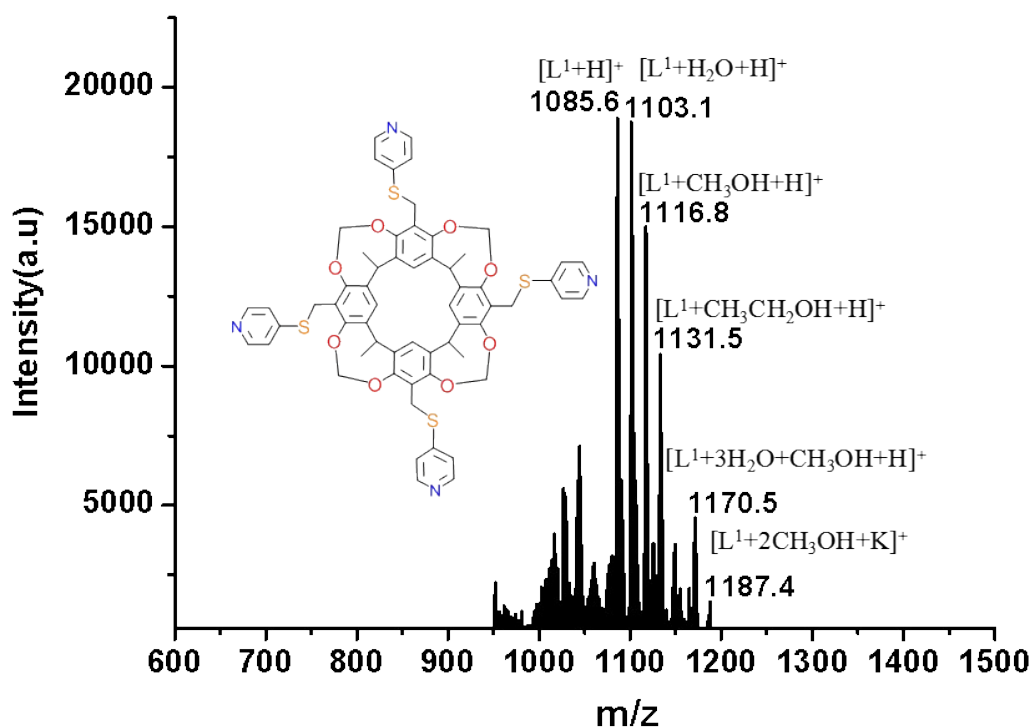
Figure S6. ESI-MS spectrum of L^1 in CH_3OH solution at 298 K.

Compound **4** (418 mg, 0.43mmol) and 2-Mercaptopyridine (208 mg, 1.87mmol) were added in acetonitrile (10 mL) and stirred at 40℃. Triethylamine (0.56 ml, 28.6mmol) was added via syringe and the solution was stirred two days. The resulting pale brown precipitate was filtered off, washed with water, acetonitrile and dried to afford the desired product as white solid (233.3 mg, 0.22 mmol) in 50% yield. ^{1}H NMR (400 MHz, DMSO-d_6, 298 K, ppm)：^{1}H NMR (400 MHz, DMSO-d_6) δ 8.47 (s, 4H), 7.68 (d, J = 35.8 Hz, 8H), 7.17 (d, J = 41.3 Hz, 8H), 5.74 (s, 4H), 4.80 (s, 4H), 4.42 (d, J = 7.9 Hz, 4H), 4.25 (s, 8H), 1.83 (s, 12H)， ^{13}C NMR (125 MHz, DMSO-d_6) δ158.31, 152.83, 149.79, 139.45, 137.15, 124.18, 122.00, 121.19, 120.41, 99.97, 31.81, 23.66, 16.57. EMS-MS (MeCN, m/z)：$[L^2+2H_2O+H]^+$, calcd for $C_{60}H_{57}N_4O_{10}S_4^+$; m/z=1121.3, found, m/z=1121; $[L^2+3H_2O+H]^+$, calcd for $C_{60}H_{59}N_4O_{11}S_4^+$, m/z=1139.31, found, m/z=1139; $[L^2+C_2H_5OH+Na]^+$, calcd for $C_{62}H_{58}N_4O_9S_4Na^+$, m/z=1153.3, found, m/z=1154; $[L^2+CH_3CN+C_2H_5OH+H]^+$,calcd for $C_{64}H_{62}N_5O_9S_4^+$, m/z=1172.3, found, m/z=1172; $[L^2+H_2O+C_2H_5OH+K]^+$,calcd for $C_{62}H_{62}N_4O_{11}S_4K^+$, m/z=1187.28, found, m/z=1187; $[L^2+2CH_3CN+K]^+$,calcd for $C_{64}H_{58}N_6O_8S_4K^+$, m/z=1205.28, found, m/z=1205.
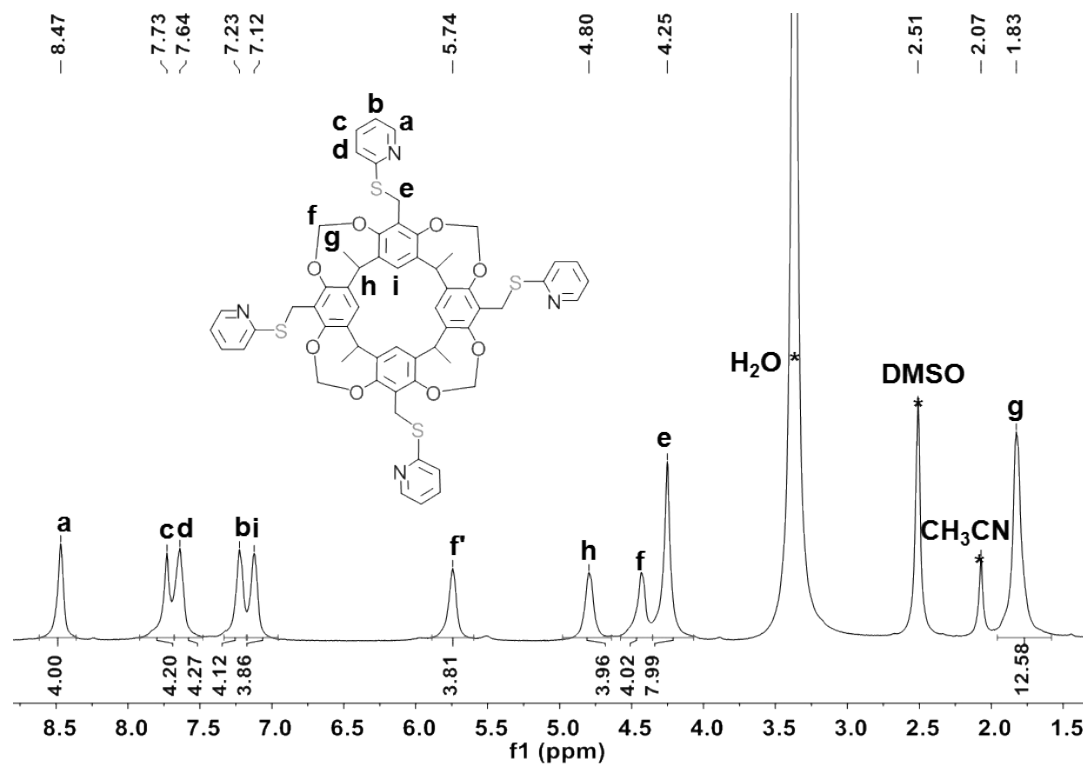
Figure S7. ^1H NMR spectrum (298 K, 400 MHz, DMSO-d_6) of **L^2**.
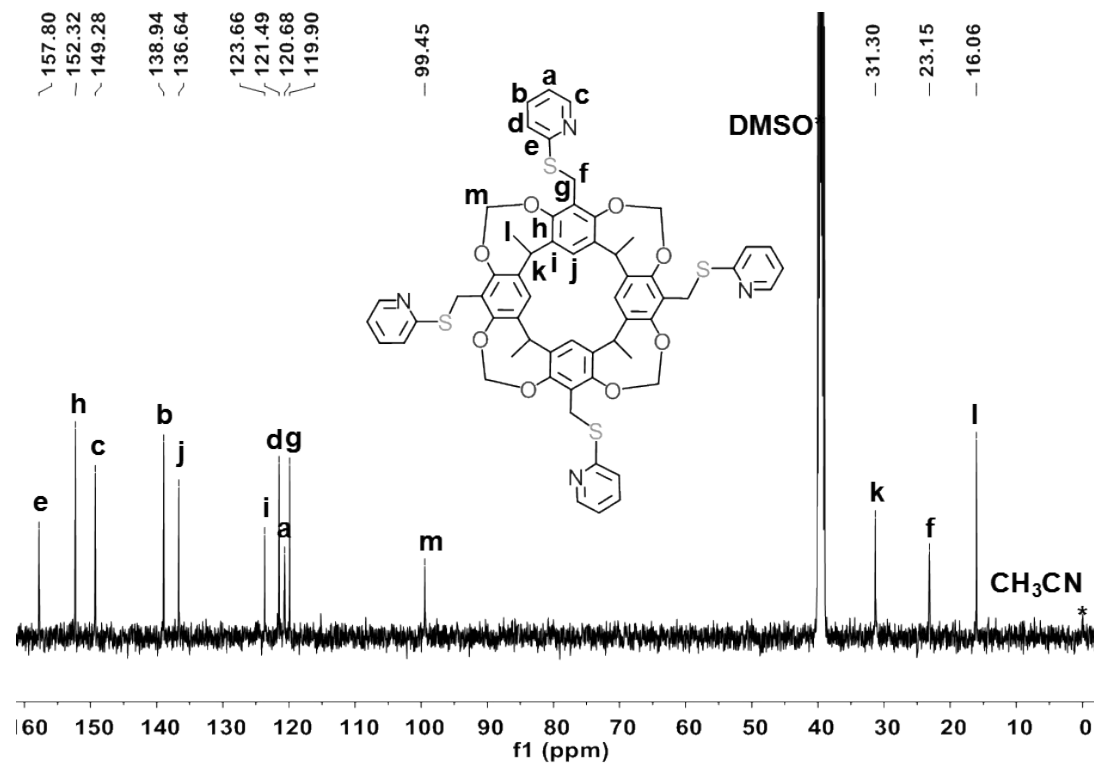
Figure S8. ^{13}C NMR spectrum (298 K, 100 MHz, DMSO-d_6) of **L^2**.
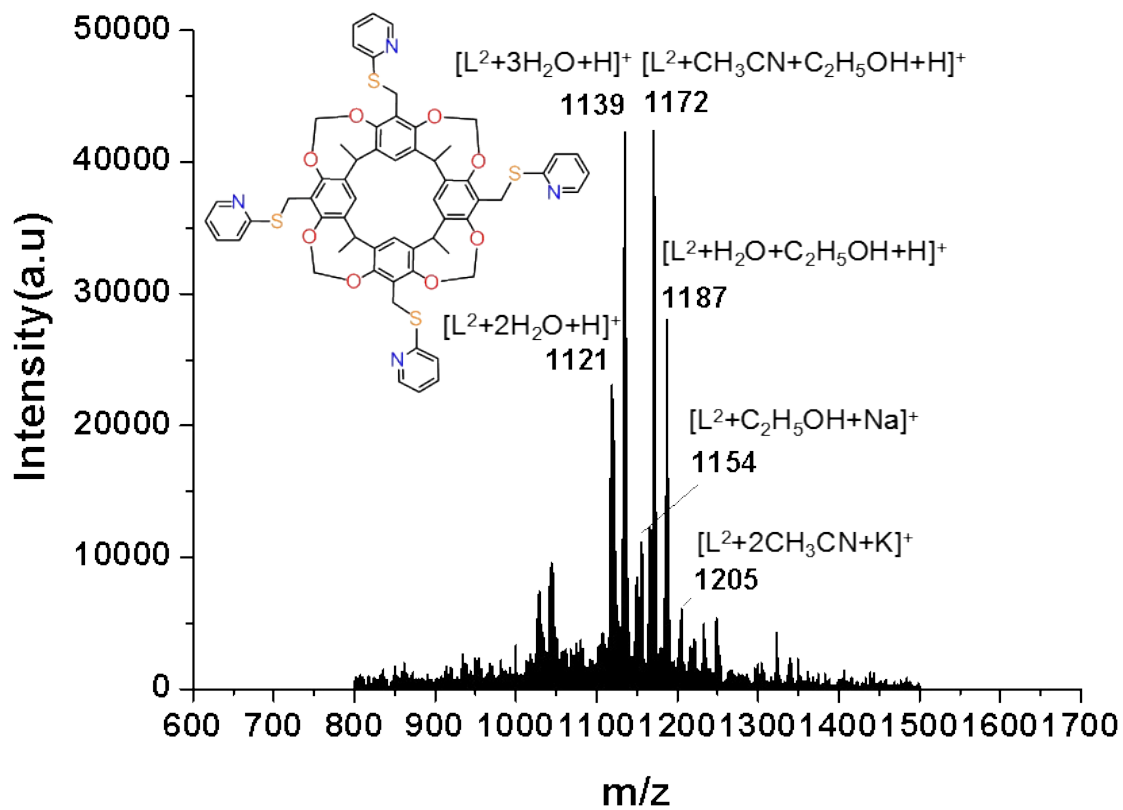
Figure S9. ESI-MS spectrum of L^2 in CH_3CN solution at 298 K.

The synthesis of MOF 1 and cluster 2.
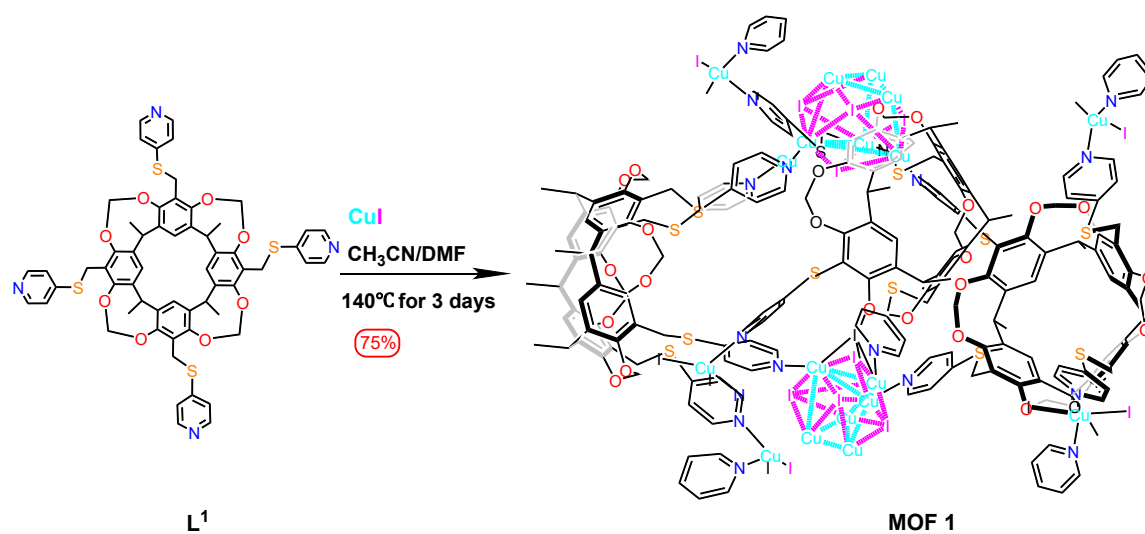
Scheme S2. Self-assembly pathway of MOF **1**.

MOF 1 ({[Cu$_6$I$_5$]$_2$[CuI$_2$]$_3$(L^1)$_3$]}$_n$): L^1 (15.0 mg, 0.013mmol) and cuprous iodide (10.5 mg,0.055mmol) were stirred in acetonitrile (1 mL) and DMF (3mL) mixture at room temperature for 3h. The mixture was then sealed in a 10 mL teflon-lined autoclave and kept at 140 °C for 72 h in an oven. Next, the reactor was slowly cooled to room temperature over 8 hours, and the high-quality yellow block single crystals of MOF **1** that were suitable for X-ray diffraction analysis were obtained (16.2mg,12.4mmol) in 63.5% yield. FT-IR (KBr, ν / cm^{-1}): 2974(C-H), 1587(C=C), 1425(Ar-H), 977(C-O), 757(C-S).
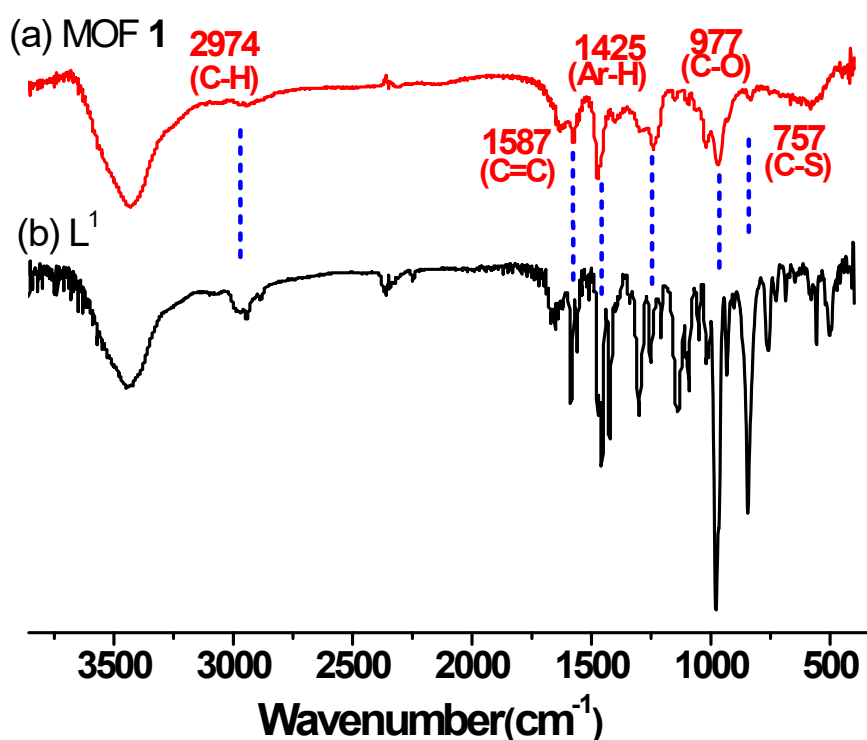
Figure S10. FT-IR spectrum of (a)MOF **1**, (b)**L^1** at 298K.
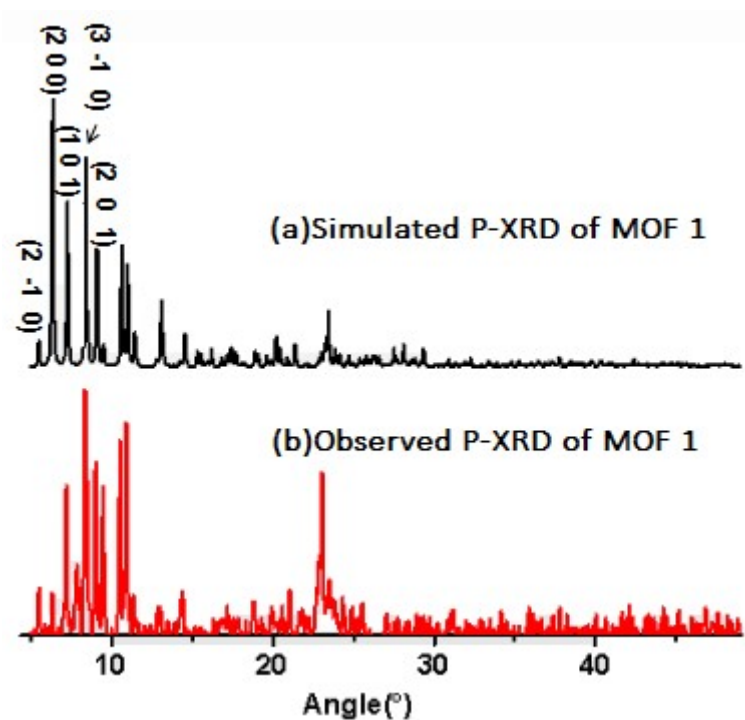
Figure S11. PXRD profiles of MOF **1**, simulated pattern (a) and observed pattern (b).
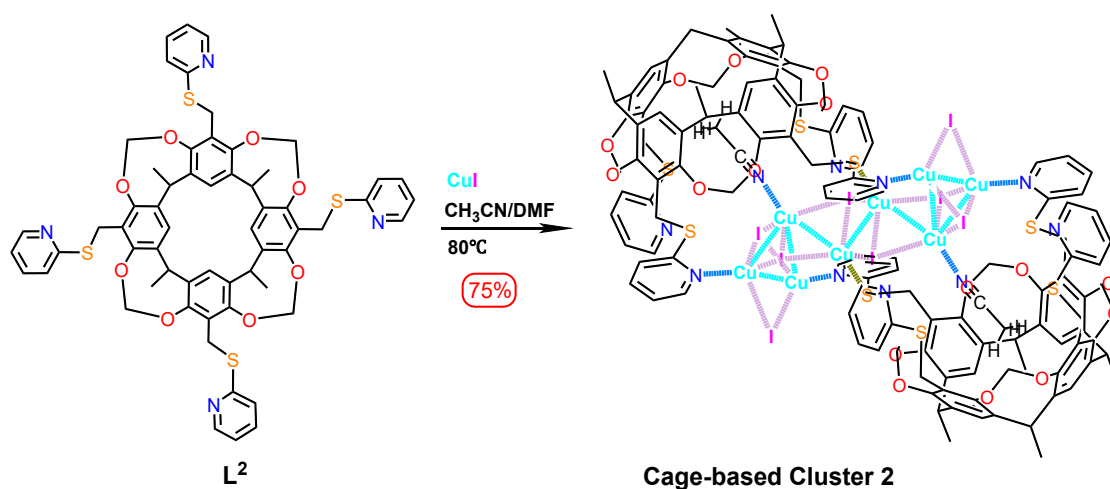
Scheme S3. Self-assembly pathway of cluster **2**

Cluster 2 ([(Cu$_8$I$_8$)L$^2_2$]): L^2 (15mg,0.013mmol) and cuprous iodide (10.5 mg,0.055mmol) were stirred in acetonitrile (2 mL) at room temperature for 8h in an assembly tube. The temperature was increased to 80°C and kept stirring for 10h. Then

1 mL DMF was added to the reaction mixture and continued for 8 hours to afford a clear yellow solution. The high-quality yellow block single crystals of cluster **2** that were suitable for X-ray diffraction analysis were obtained by slow diffusion of diethyl ether into their 2:1 CH$_3$CN/DMF (v/v, 3mL) solution for 54 h (36.8 mg, 8.5 mmol) in 75% yield.

^{1}H NMR (400 MHz, DMSO-d_6) δ 8.48 (s, 2H), 7.72 (s, 2H), 7.64 (s, 1H), 7.23 (s, 1H), 5.73 (s, 1H), 4.77 (s, 1H), 4.41 (s, 1H), 4.24 (s, 4H), 2.89 (s, 1H), 2.73 (s, 1H), 2.07 (s, 1H), 1.81 (s, 3H). ^{13}C NMR (100 MHz, DMSO) δ 158.26, 152.81, 149.75, 139.43, 137.14, 124.14, 121.18, 99.94, 40.91, 40.71, 40.50, 40.29, 40.08, 39.87, 39.66, 36.27, 31.80, 23.64, 16.56. MALDI-TOF-MS (CH$_3$CN, m/z)：[cluster **2-L^2-**7CuI+4H$_2$O+Na]$^+$, calcd for C$_{60}$H$_{60}$CuIN$_4$NaO$_{12}$S$_4^+$; 1369.5, found, 1369.1；[cluster **2-L^2**-6CuI-I+4CH$_3$CN+3H$_2$O]$^+$, calcd for C$_{68}$H$_{70}$Cu$_2$IN$_8$O$_{11}$S$_4^+$, 1555.2, found, 1555.1; [cluster **2-L^2**-4CuI-I+DMSO+3H$_2$O]$^+$, calcd for C$_{62}$H$_{64}$Cu$_5$I$_4$N$_4$O$_{12}$S$_5^+$, 2038.5, found, 2038; [cluster **2**-8CuI+3H$_2$O+H]$^+$, calcd for C$_{120}$H$_{111}$N$_8$O$_{19}$S$_8^+$, 2223, found, 2223.5; [cluster **2**-7CuI+CH$_3$OH+Na]$^+$, calcd for C$_{121}$H$_{108}$CuIN$_8$NaO$_{17}$S$_8^+$, 2413.38, found, 2413; [Cluster **2**-7CuI+CH$_3$OH+H$_2$O+CH$_3$CN+Na]$^+$, calcd for C$_{123}$H$_{113}$Cu$_2$I$_2$N$_9$NaO$_{18}$S$_8^+$, 2472, found, 2472.4; [cluster **2**-6CuI+Na]$^+$, calcd for C$_{120}$H$_{113}$Cu$_2$I$_2$N$_8$NaO$_{16}$S$_8^+$, 2571, found, 2571.2; [cluster **2**-6CuI+CH$_3$OH+H$_2$O+Cu]$^+$, calcd for C$_{121}$H$_{110}$Cu$_3$I$_2$N$_8$O$_{18}$S$_8^+$, 2661, found, 2661.2; [cluster **2**-6CuI+2DMSO+Na]$^+$, calcd for C$_{124}$H$_{116}$Cu$_2$I$_2$N$_8$NaO$_{18}$S$_{10}^+$, 2728, found, 2728.2; [cluster **2**-5CuI+Na]$^+$, calcd for C$_{120}$H$_{104}$Cu$_3$I$_3$N$_8$NaO$_{16}$S$_8^+$, 2761, found, 2761; [cluster **2**-5CuI+Cu]$^+$, calcd for C$_{120}$H$_{104}$Cu$_4$I$_3$N$_8$O$_{16}$S$_8^+$, 2801, found, 2801; [cluster **2**-5CuI+H$_2$O+DMSO+Cu]$^+$ calcd for C$_{122}$H$_{112}$Cu$_4$I$_3$N$_8$O$_{18}$S$_9^+$, 2896, found, 2896.
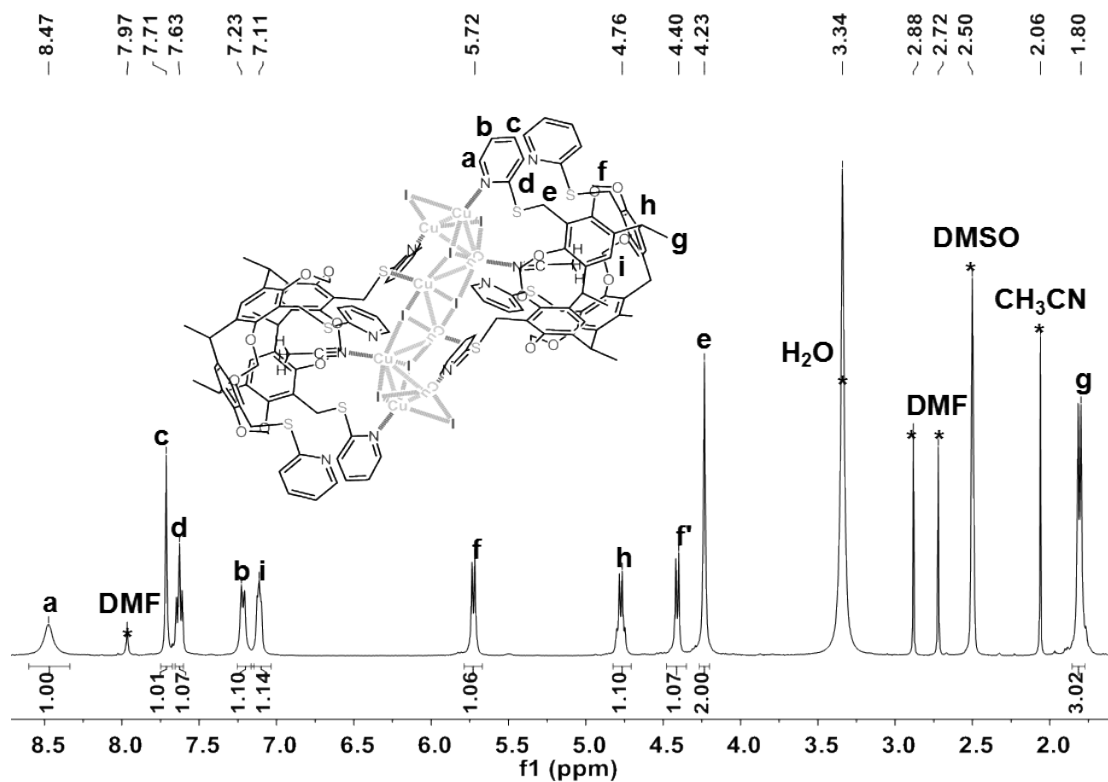
Figure S12. ^{1}H NMR spectrum (298 K, 400 MHz, DMSO-d_6) of cluster **2**
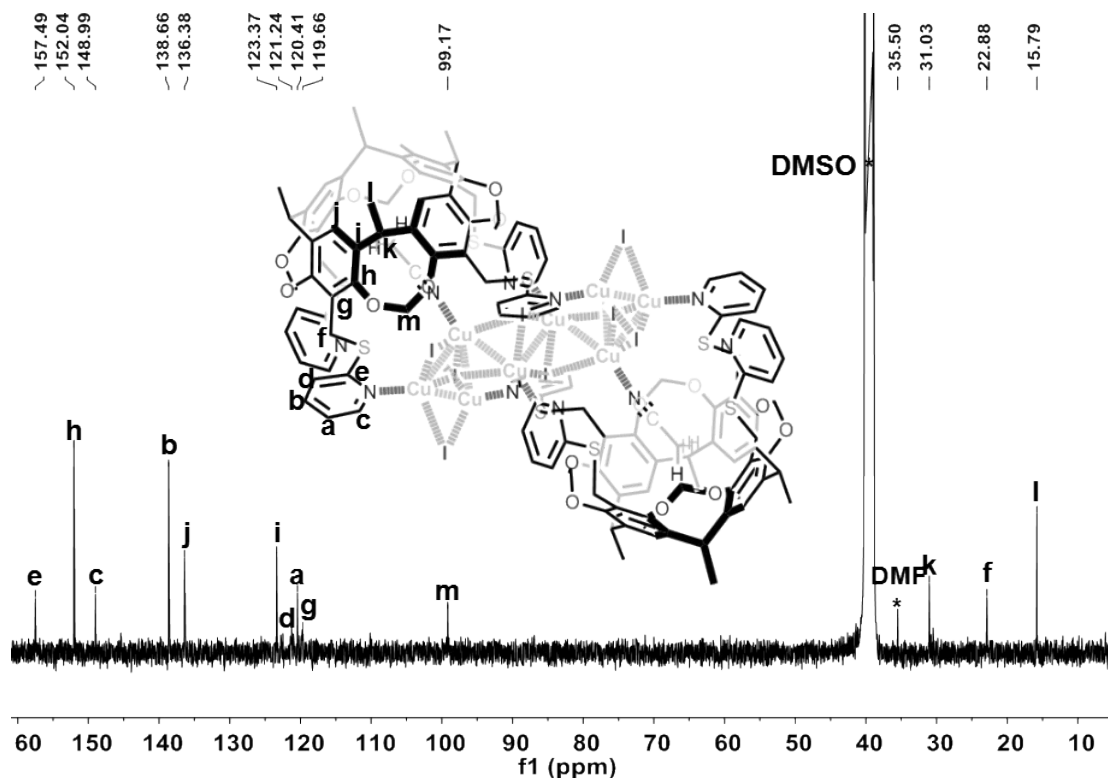
Figure S13. ^{13}C-NMR spectrum (100MHz, DMSO-d_6) of cluster **2** recorded at 298 K.
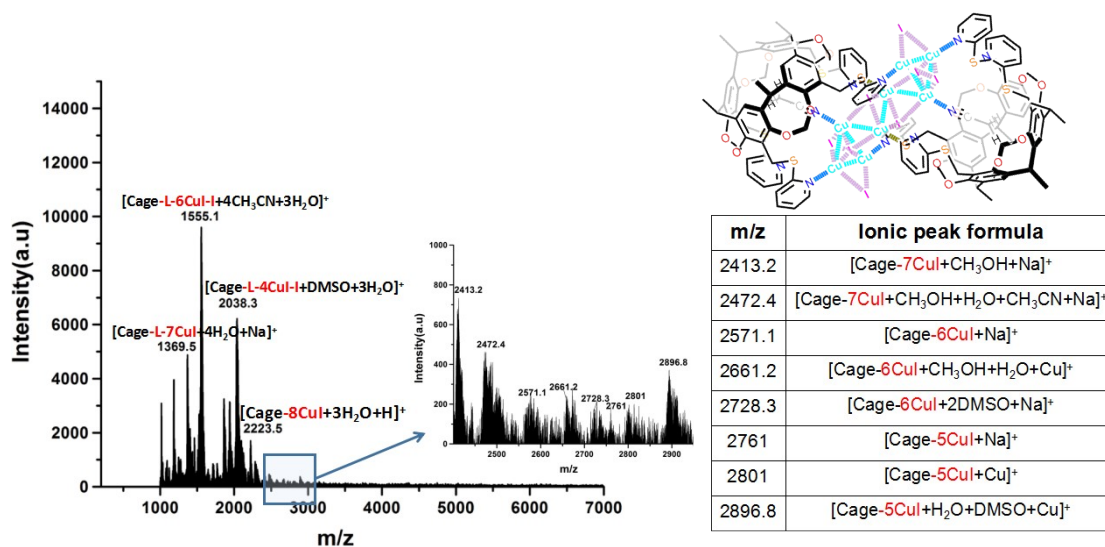
Figure S14. MALDI-TOF-MS spectrum of cluster **2**.

m/z	Ionic peak formula
2413.2	[Cage-7CuI+CH$_3$OH+Na]$^+$
2472.4	[Cage-7CuI+CH$_3$OH+H$_2$O+CH$_3$CN+Na]$^+$
2571.1	[Cage-6CuI+Na]$^+$
2661.2	[Cage-6CuI+CH$_3$OH+H$_2$O+Cu]$^+$
2728.3	[Cage-6CuI+2DMSO+Na]$^+$
2761	[Cage-5CuI+Na]$^+$
2801	[Cage-5CuI+Cu]$^+$
2896.8	[Cage-5CuI+H$_2$O+DMSO+Cu]$^+$
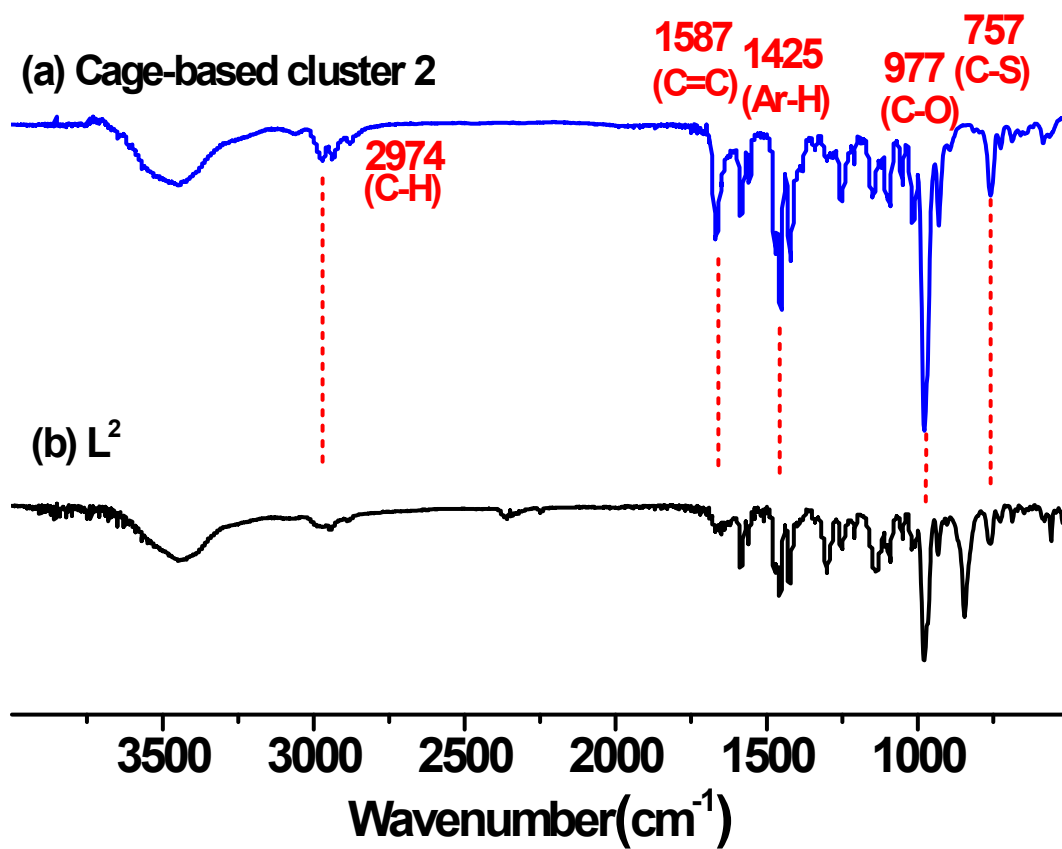
Figure S15. FT-IR spectrum of (a) cluster **2**, (b) **L^2** at 298K.
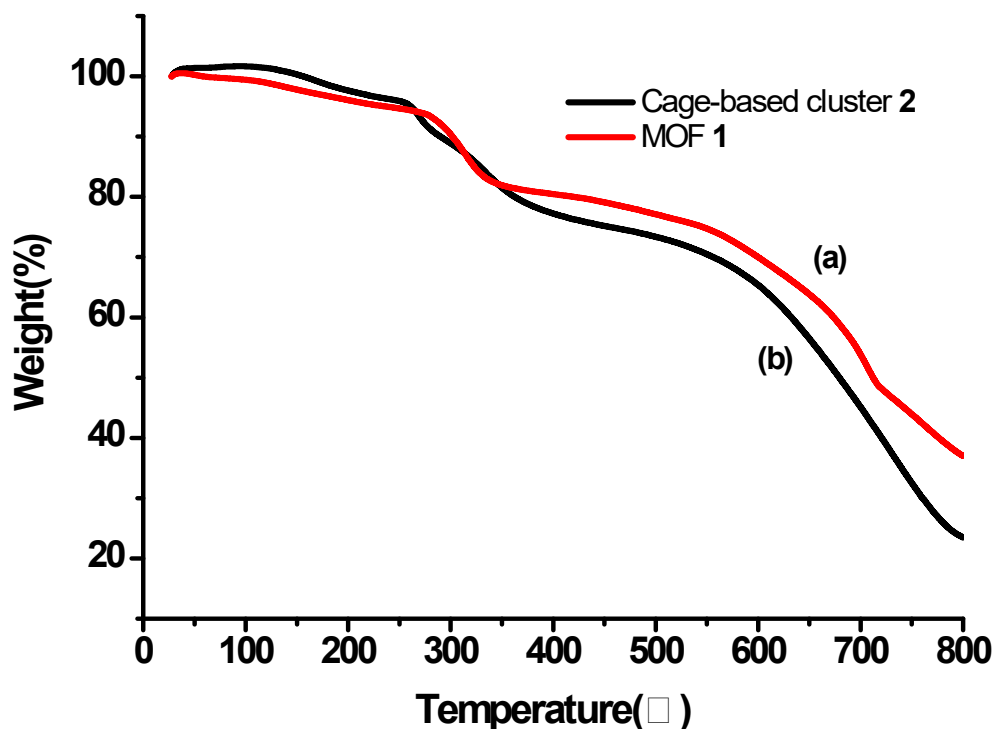
Figure S16. TGA profiles of (a) MOF **1**, (b) cluster **2** recorded under a nitrogen atmosphere.

S3. X-ray crystallography

X-ray diffraction measurements were carried out at 291 K on a Bruker Smart Apex CCD area detector equipped with a graphite monochromated MoKα radiation (λ= 0.71073 Å). The absorption correction for all complexes was performed using SADABS. All the structures were solved by direct methods and refined employing full-matrix least-squares on F^2 by using SHELXTL (Bruker, 2000) program and expanded using Fourier techniques. All non-H atoms of the complexes were refined with anisotropic thermal parameters. The hydrogen atoms were included in idealized positions.   Final residuals along with unit cell, space group, data collection, and refinement parameters are presented in Table S1-S3.

Table S1. Crystal structure determination data for MOF **1** and cluster **2**.

Crstal name	MOF **1**	Cluster **2**
Formula	$C_{360}H_{312}Cu_{15}I_{19}N_{24}O_{48}$	$C_{124}H_{110}Cu_8I_8N_{10}O_{16}$
Formula weight	9876.14	3776.31
Color	Yellow	Yellow
Crystal system	hexagonal	monoclinic
Space group	P63/m	P21/n
a (Å)	32.1757(18)	21.5046(17)
b (Å)	32.1757(18)	16.0447(6)
c (Å)	13.5257(11)	23.0476(14)
α	90	90
β	90	115.557(9)
γ	120	90
Volume ($Å^3$)	12126.8(17)	7174.2(9)
Z	1	2
No.of unique	9829	17265
No.of parameters	6094	9481
Final R indices	$R_1 = 0.1534$	$R_1 = 0.0605$

Table S2. Bond distances (Å) and angles (°) in the crystal structures of MOF **1.**

Bond	Dist.[Å]	Bond	Dist.[Å]
I3-Cu2A	2.5098	I3-Cu2	2.7910
Cu1-N1	2.0543	Cu1-Cu1A	2.4302
Cu1-Cu1A	2.7321	Cu1-I1	2.6808
Cu1-Cu1	2.7502	Cu1-I2	2.5630
C27-Cu1A	2.5431	N2-Cu2A	2.1807
N2-Cu2	2.1392	Cu2A-Cu2	1.4364
Cu2A-N1AA	2.4231	Cu2A-I5	2.4929
Cu2A-N2	2.1807	Cu2-I5	2.6619
Cu2-Cu2	2.7511	Cu2-C2AA	2.3715
Cu2-I4	2.7626	N2A-Cu1A	2.1540

Bond	Angel[°]	Bond	Angel[°]
Cu2A-I3-Cu2	30.87	Cu2-I3-Cu2	59.06
N1-Cu1-Cu1A	77.92	N1-Cu1-I2	105.02
N1-Cu1-I1	104.07	N1-Cu1-Cu1	138.26
N1-Cu1-Cu1A	94.83	N1-Cu1-I2	110.67
N1-Cu1-Cu1	112.05	Cu1A-Cu1-I2	60.61
Cu1A-Cu1-I1	64.29	Cu1A-Cu1-Cu1	60.34
Cu1A-Cu1-Cu1	112.05	Cu1A-Cu1Cu1A	121.82
I2-Cu1-I1	108.58	I2-Cu1-Cu1	55.74
I2-Cu1-Cu1A	159.82	I2-Cu1-I2	113.83
I1-Cu1-Cu1	59.14	Cu1-Cu1-Cu1	60.00
Cu1-Cu1-Cu1A	106.42	Cu1-Cu1-I2	111.05
Cu1-Cu1-Cu1	90.00	Cu1-Cu1-Cu1A	53.77
Cu1A-Cu1-I2	60.69	I5-Cu2A-N2	115.74
I5-Cu2A-Cu2	80.42	I5-Cu2A-N1AA	107.46
Cu2-Cu2A-N2	69.02	Cu2-Cu2A-N1A	50.04

N2-Cu2A-N1AA	18.98	I3-Cu2-N2	96.59
C32-N2-Cu2	114.18	C2AA-I4-Cu2	58.05
S2-I4-Cu2	101.68	H32-I4-Cu2	80.25
H2AA-I4-Cu2	22.16	N1AA-N2-Cu2A	97.99

Table S3. Bond distances (Å) and angles (°) in the crystal structures of cluster **2**

Bond	Dist.[Å]	Bond	Dist.[Å]
I1-Cu5	2.6330(2)	Cu8-N2	2.0078(2)
I1-Cu6	2.6680(2)	I4-Cu7	2.5029(2)
I1-Cu5	2.7295(2)	I4-Cu8	2.8592(2)
I2-Cu5	2.6042(2)	Cu5-S1	2.3691(2)
I2-Cu6	2.6639(2)	Cu6-N3	2.0433(2)
I2-Cu8	2.5697(2)	Cu7-N1	2.0036(2)
I3-Cu6	2.6389(2)	I3-Cu8	2.8046(2)
Cu1-Cu1	2.750(7)	Cu1-Cu1	2.821(8)
Bond	Angel[°]	Bond	Angel[°]
Cu5-I1-Cu6	67.25(1)	I3-Cu8-I4	103.04(1)
Cu5-I1-Cu5	62.49(1)	I3-Cu8-N2	97.85(1)
Cu5-a-I1 -Cu6	111.77(1)	I4-Cu8-N2	107.16(1)
Cu5-I2-Cu6	67.72(1)	Cu5-S1-C9	100.42(1)
Cu5-I2-Cu8	107.17(1)	Cu5-S1-C10	107.07(1)
Cu6-I2-Cu8	63.28(1)	Cu6-I3-Cu7	68.71(1)
Cu6-I3-Cu8	60.51(1)	C54-S11-C55	104.84(1)
Cu7-I3-Cu8	55.97(1)	Cu7-I4-Cu8	56.48(1)
I1-Cu5-I2	110.39(1)	I1-Cu5-S1	103.55(1)
I1-Cu5 -I1	117.51(1)	I2-Cu5-S1	122.76(1)
I1-a-Cu5-I2	97.99(1)	I1-a-Cu5-S1	105.45(1)
I1-Cu6-I2	107.52(1)	Cu7-N1-C10	123.00(1)
I1-Cu6-I3	116.44(1)	Cu7-N1-C11	117.05(1)
I1-Cu6-N3	106.10(1)	I2-Cu6-I3	118.73(1)
I2-Cu6-N3	107.63(1)	I3-Cu6-N3	99.03(1)
Cu8-N2-C55	127.33(1)	I3-Cu7-I4	119.32(1)
Cu8-N2-C57	115.77(1)	I3-Cu7-N1	104.18(1)
Cu6-N3-C58	165.98(1)	I4-Cu7-N1	129.01(1)
I2-Cu8-I3	116.13(1)	I2-Cu8-I4	99.00(1)
I2-Cu8-N2	130.74(1)		
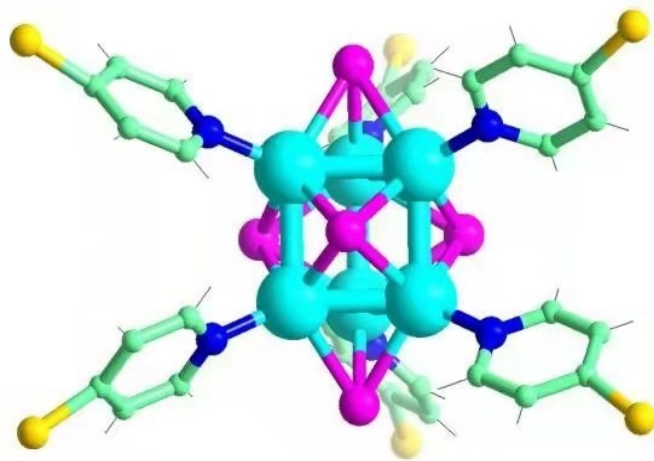
Figure S17. The X-ray single crystal diffraction photograph of MOF **1**.
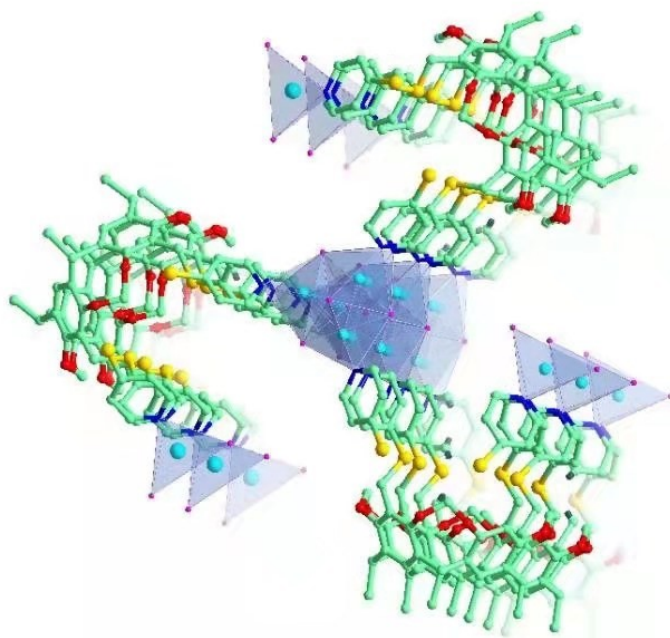
Figure S18. The X-ray single crystal diffraction photograph of MOF **1**. viewing along the c axes.
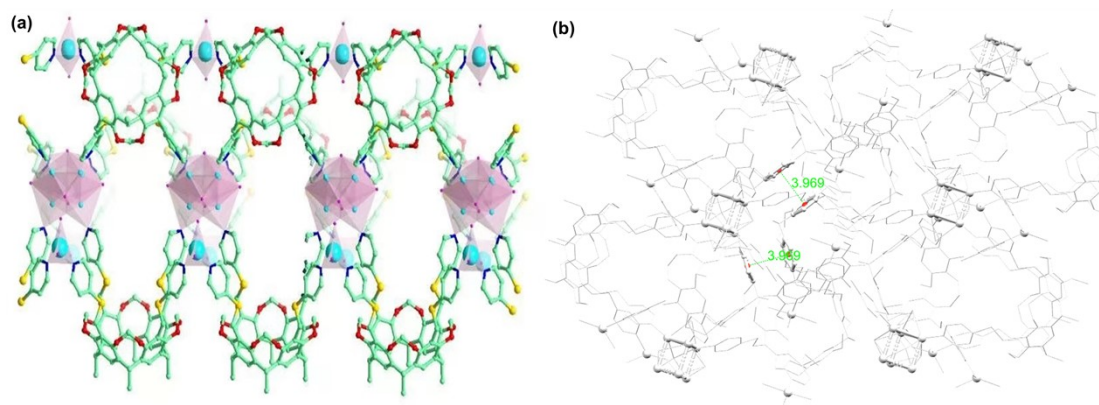
Figure S19. Packing of a 3-D molecular arrays in the crystal structure of MOF **1** viewing along *a* axis. (a) 1D cage-based coordination polymer structure; (b) the week π…π interactions between phenyl groups in the crystal state.
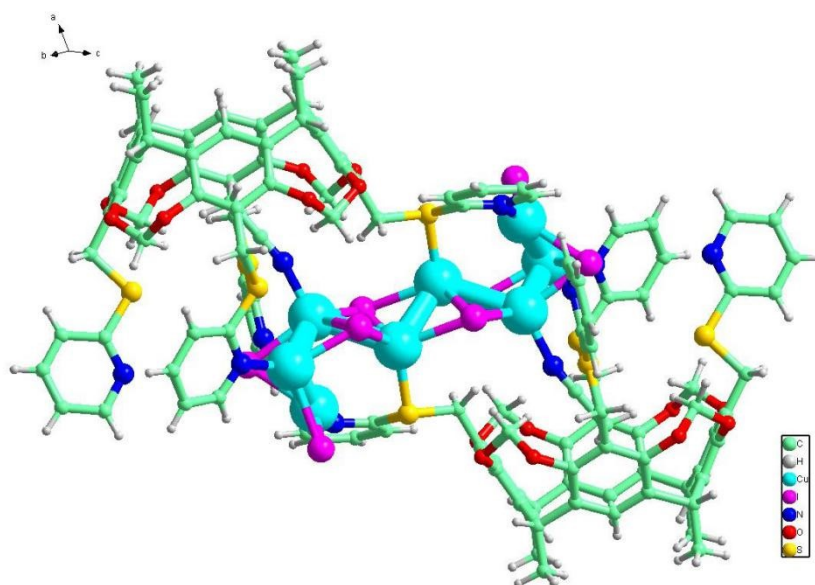
Figure S20. The X-ray single crystal diffraction photograph of cluster **2**.
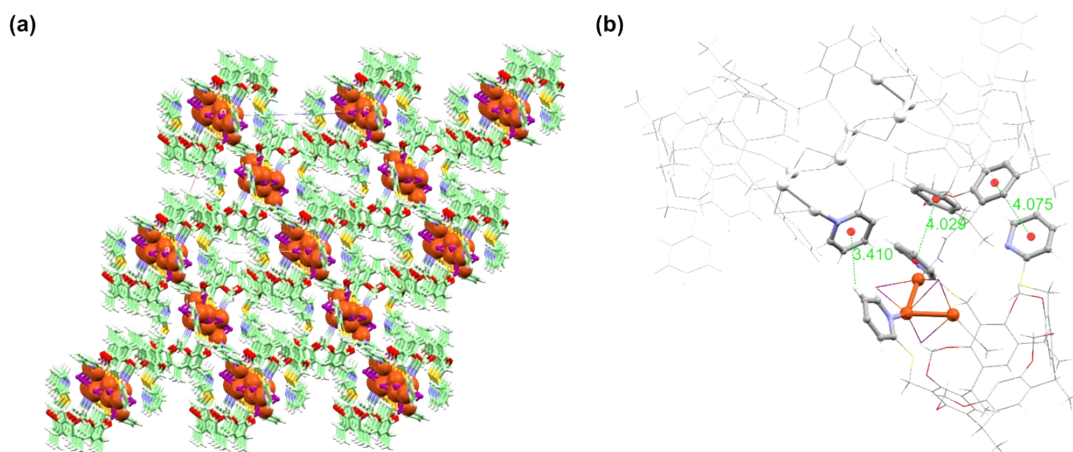
Figure S21. Packing of a 3-D molecular arrays in the crystal structure of cluster **2** viewing along the b axes. (a) stacking structures; (b) the C-H···π and π···π interactions modes observed in the crystal structure.

S4. Photophysical data of MOF 1 and Cluster 2

Table S4. Photophysical data of MOF **1** and Cluster **2**

Sample	Medium (T/K)	Uv-vis Absorbance λ /nm (ε/M^{-1} cm^{-1})	Excitation λ /nm	Emission λ/nm	Lifetime (us)	Quantum Yield (%)
MOF **1**	Solid (298)	268 318	468 555	648	0.32	8
Cluster **2**	DMSO (298)	285(16088) 310(19228)	453	506	6.34	1.1
	Solid (298)	295	400	605	136.4	9
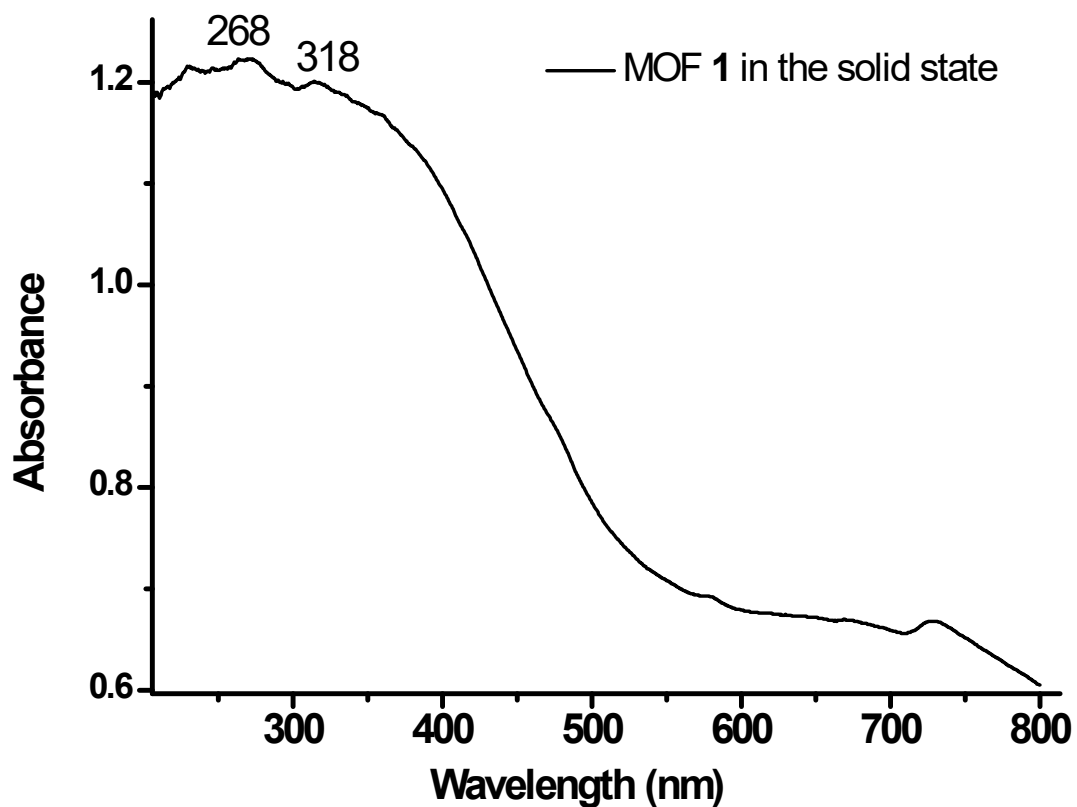
Figure S22. UV-Vis absorption spectrum of MOF **1** in the solid state.
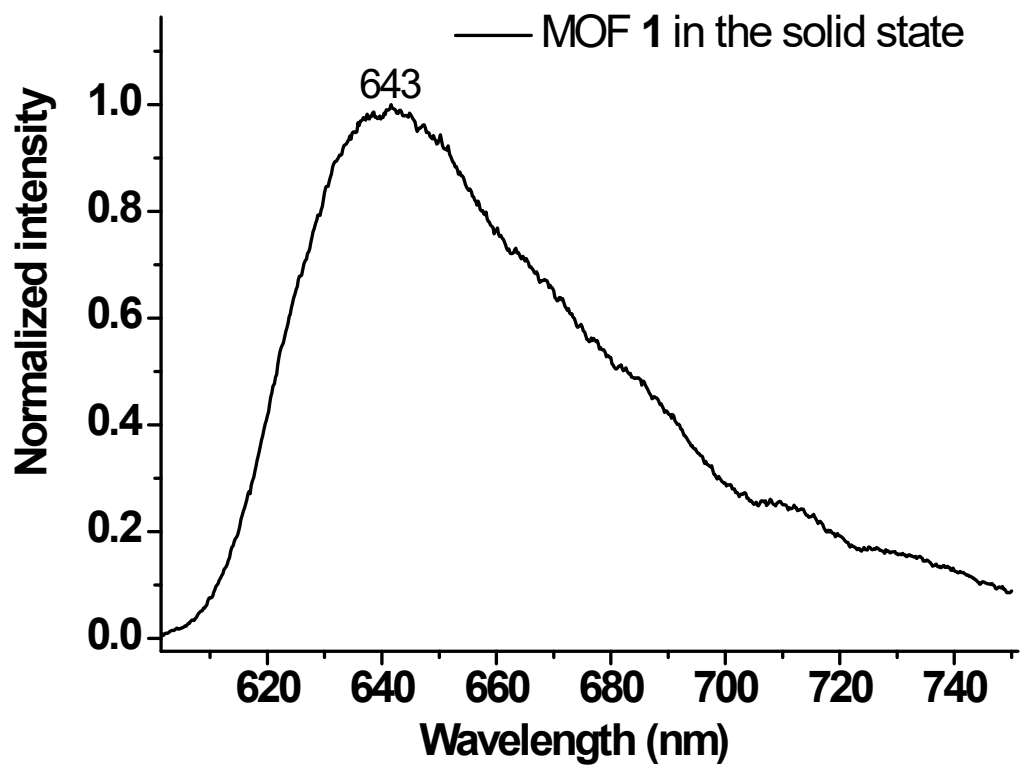
Figure S23. Emission spectra of MOF **1** in the solid state at 298k: (a)555 excitation; (a)468 excitation.
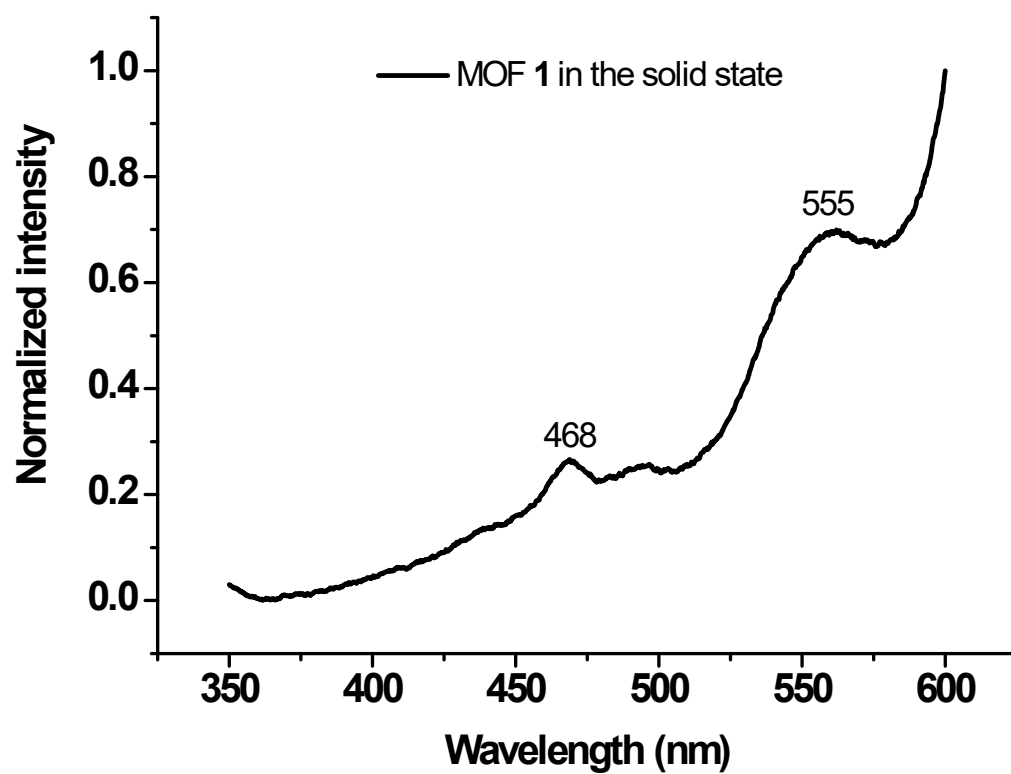
Figure S24. Excitation spectra of MOF **1** in the solid state at 298k.
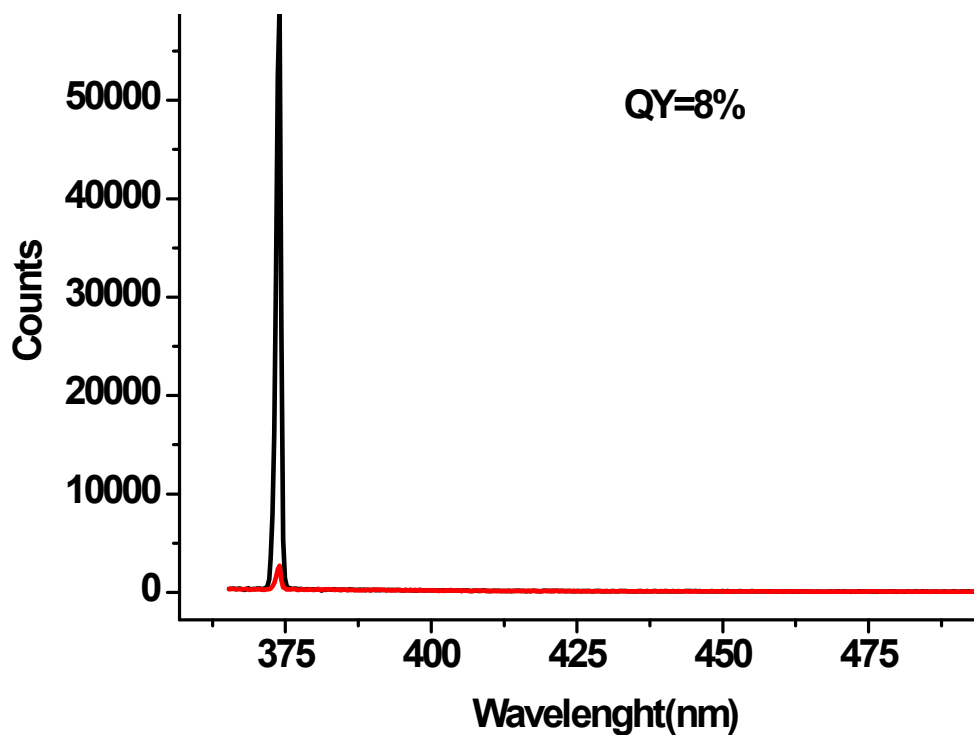
Figure S25. Quantum yield spectra of MOF **1** in the solid state at 298k.

Model	ExpDec1		
Equation	y = A1*exp(-x/t1) + y0		
Reduced Chi-Sqr	1918.82416		
Adj. R-Square	0.98362		
		Value	Standard Erro
B	y0	16.95863	0.49523
B	A1	11488.8944	22.71595
B	t1	0.31925	9.29375E-4
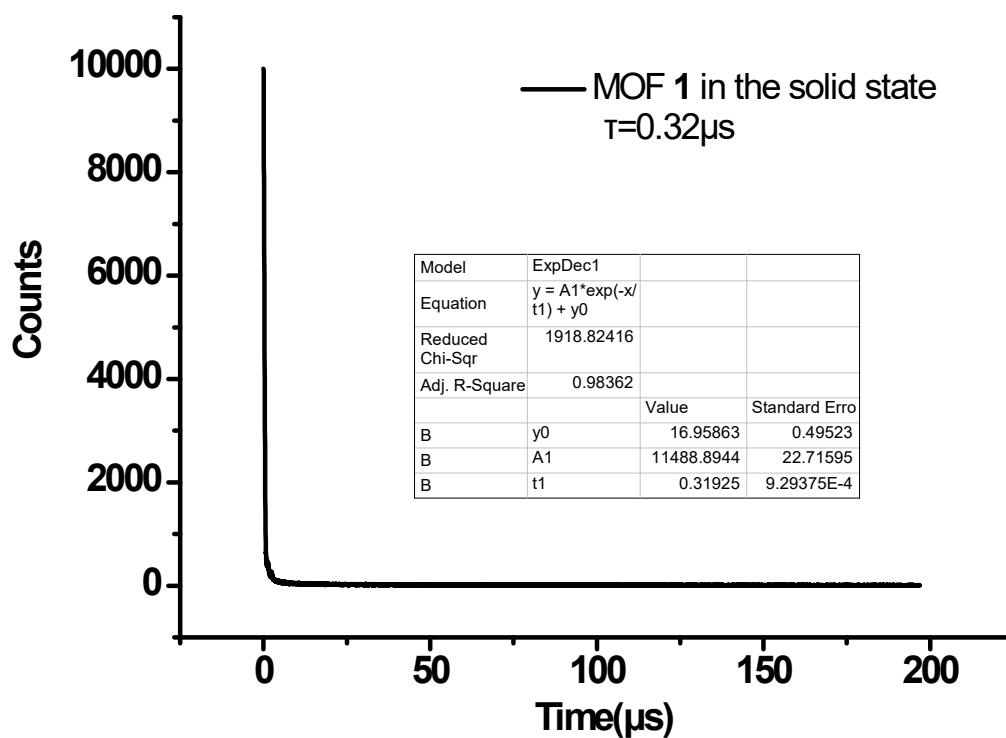
Figure S26. Phosphorescence decay profiles of MOF **1** in the solid state at 298k.
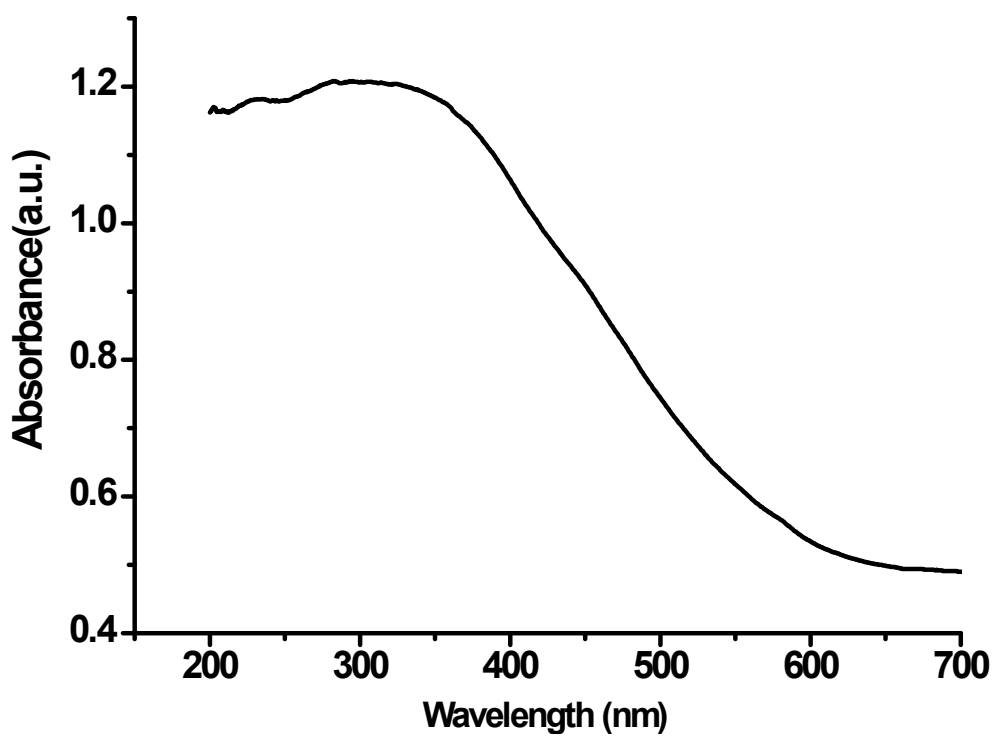
Figure S27. UV-Vis absorption spectrum of cluster **2** in the solid state.
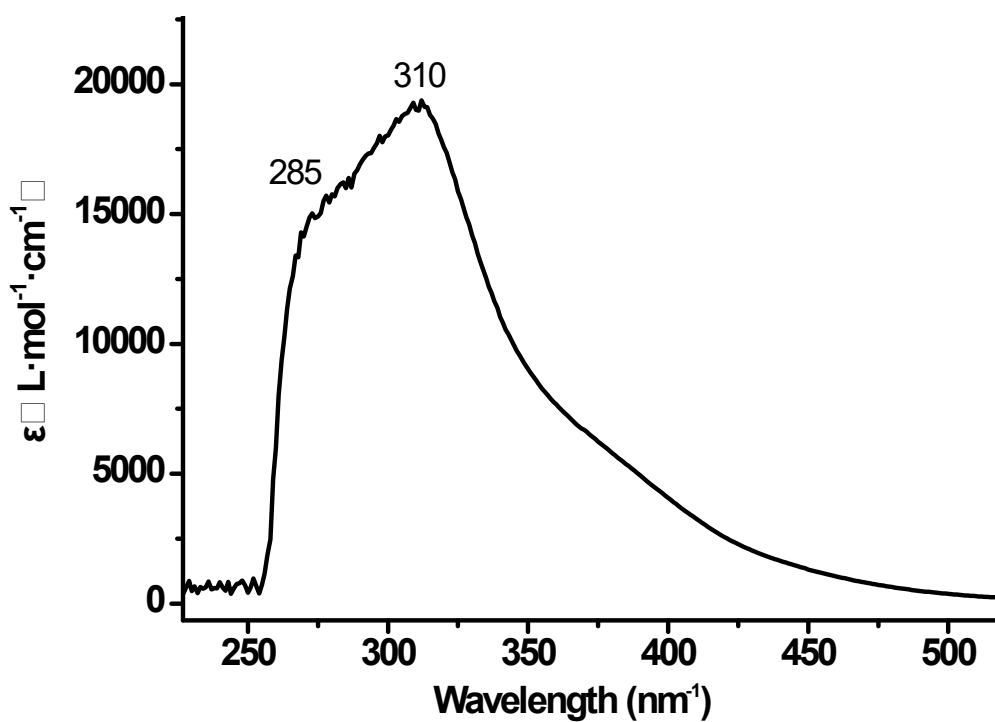
Figure S28. UV-Vis absorption spectrum of cluster **2** in DMSO solution (1×10^{-4}mol/L).
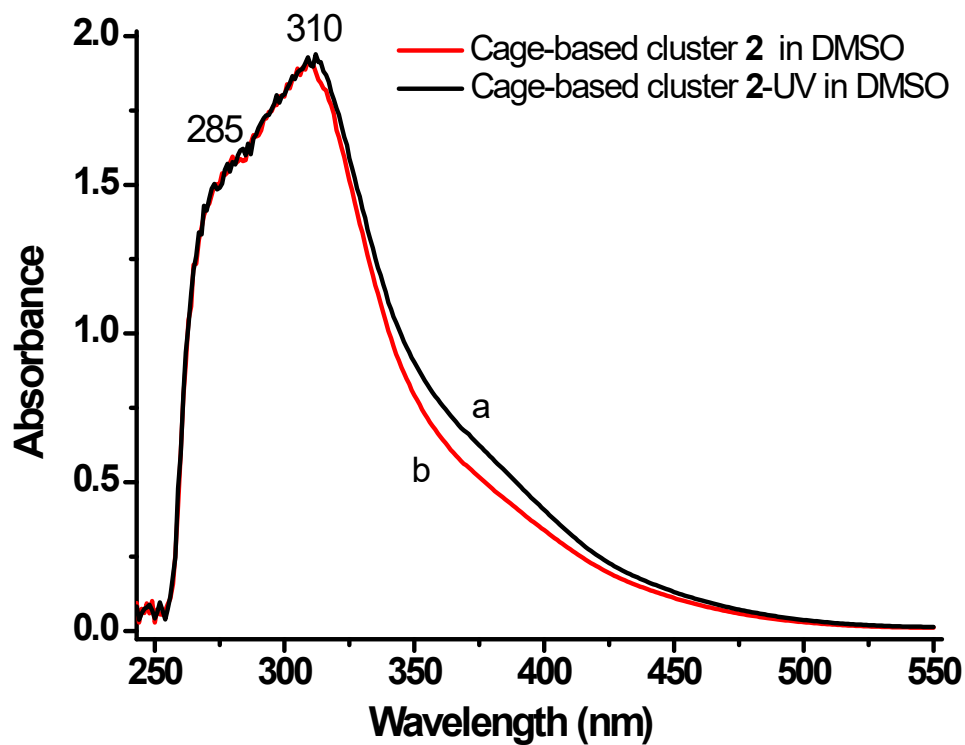
FigureS29.UV-Vis absorption spectrum of cluster **2** in DMSO solution (1×10^{-4} mol/L): (a) no treatment; (b) after UV irradiation.
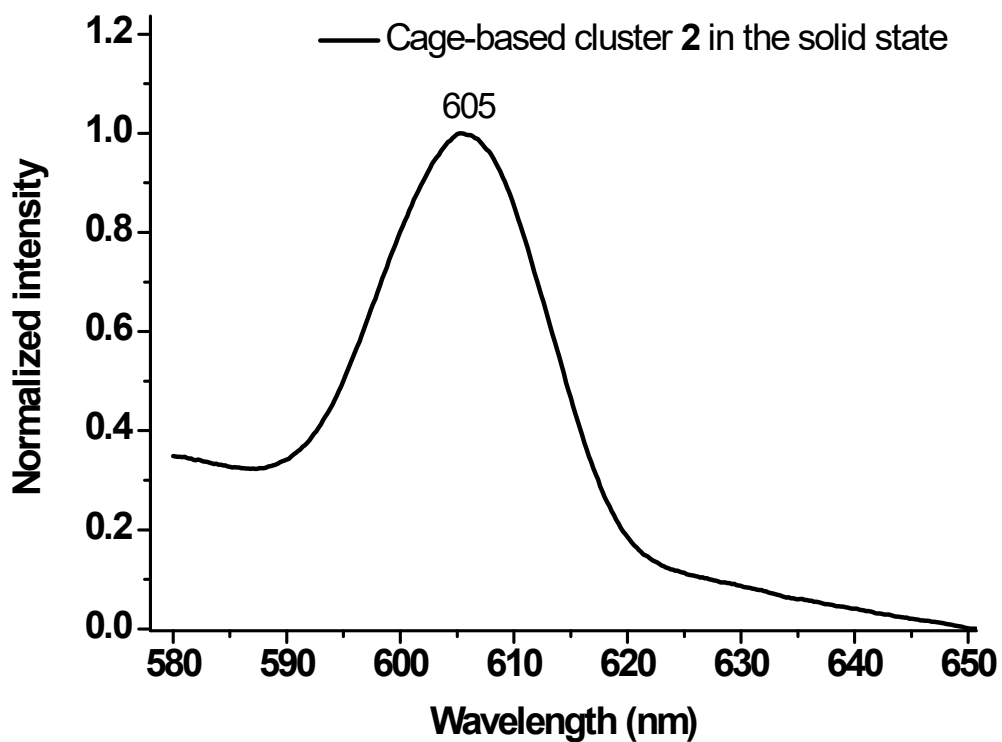
Figure S30. Emission spectra of cluster **2** in the solid state at 298k.
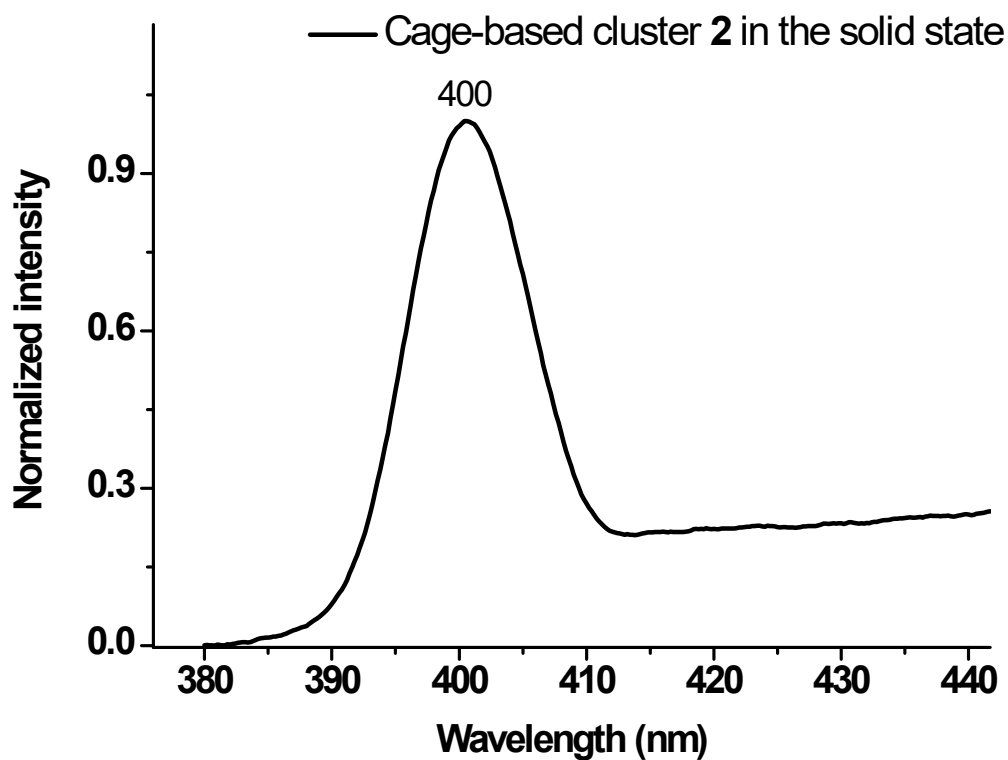
Figure S31. Excitation spectra of cluster **2** in the solid state at 298k.
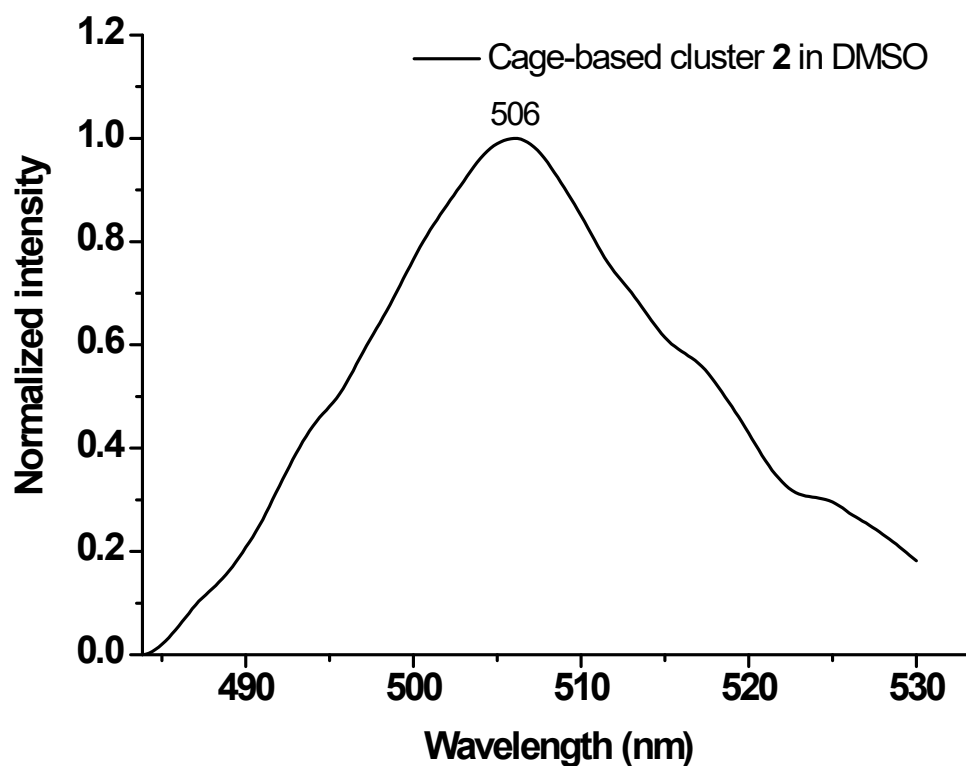
Figure S32. Emission spectra of Cluster **2** in DMSO 298k.
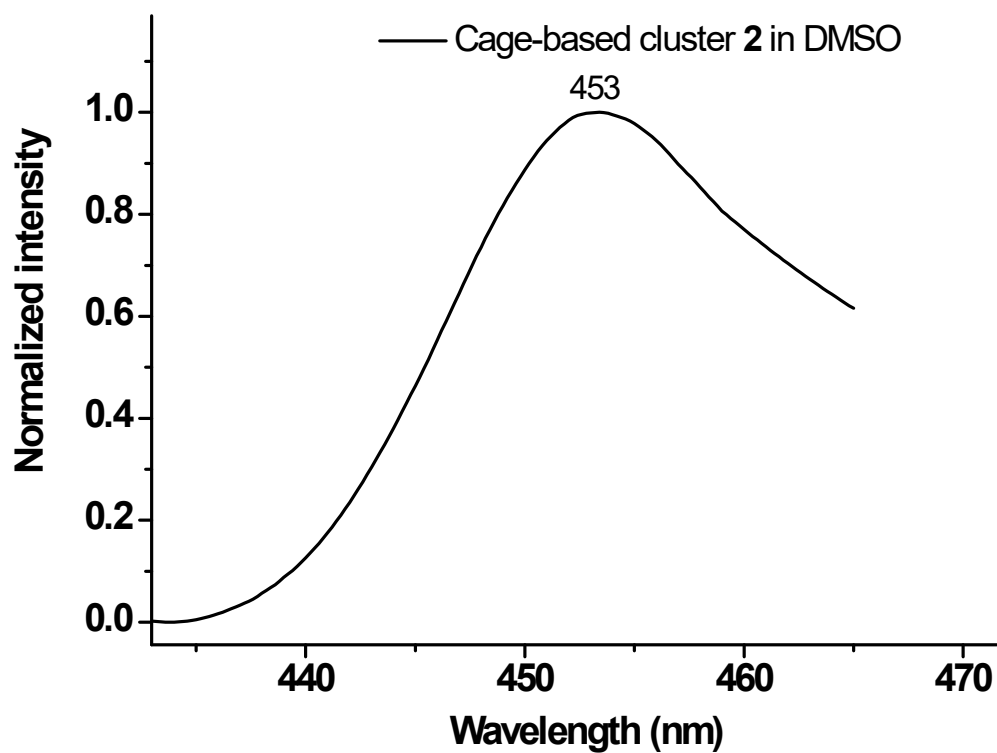
Figure S33. Excitation spectra of cluster **2** in DMSO at 298k.

Model	ExpDec3		
Equation	y = A1*exp(-x/t1) + A2*exp(-x/t2) + A3*exp(-x/t3) + y0		
Reduced Chi-Sqr	78.2315		
Adj. R-Square	0.99772		
		Value	Standard Error
HCX-1-Decay	y0	0.19592	0.22137
HCX-1-Decay	A1	842.77734	20.15807
HCX-1-Decay	t1	7.80496	0.28496
HCX-1-Decay	A2	17.59851	12.03729
HCX-1-Decay	t2	38.47468	17.12513
HCX-1-Decay	A3	4302.83216	24.89677
HCX-1-Decay	t3	1.50921	0.01127
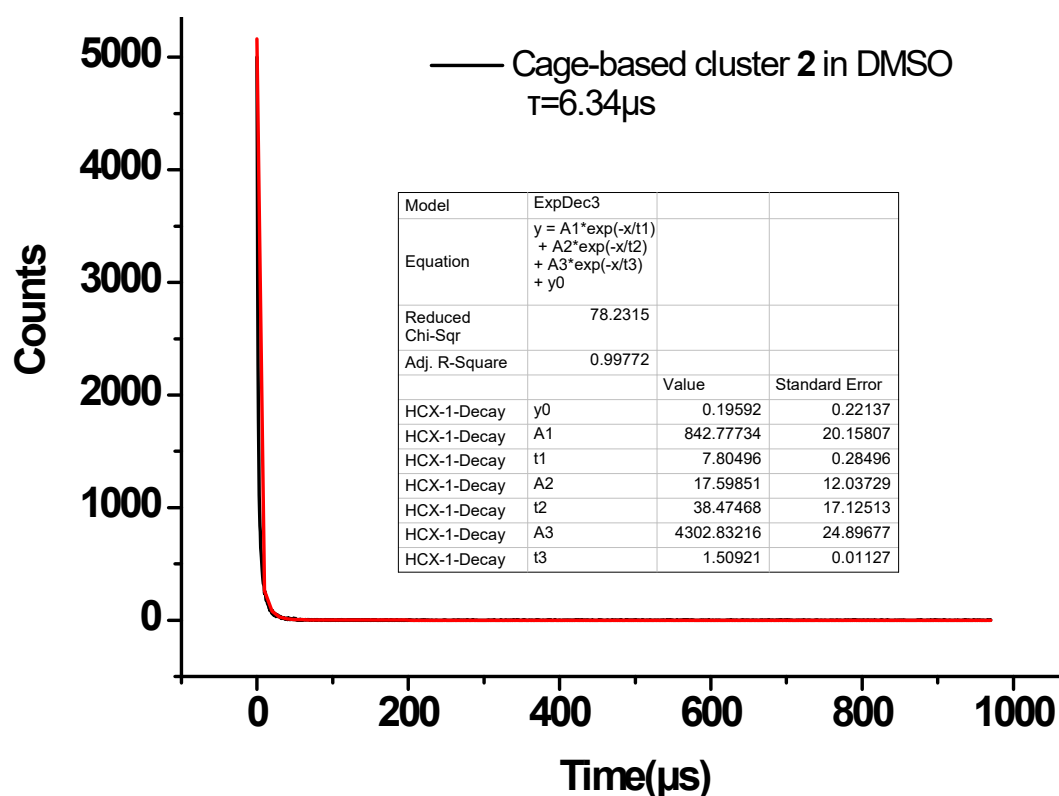
Figure S34. Phosphorescence decay profiles of cluster **2** in DMSO at 298k.
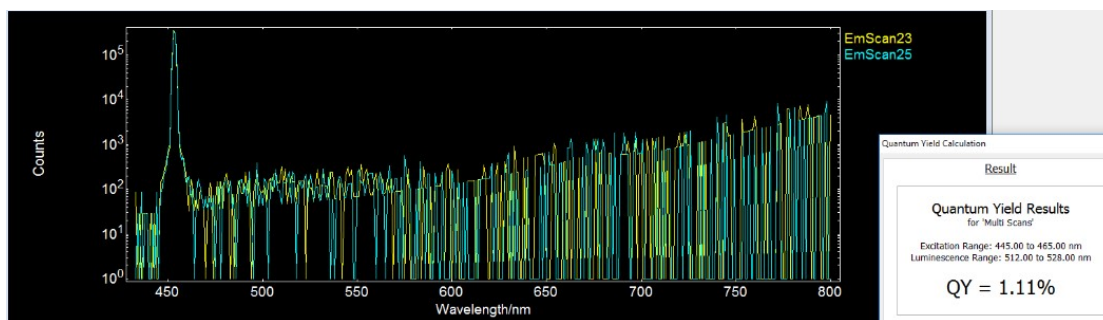
Figure S35. Quantum yield spectra of cluster **2** in DMSO at 298k.
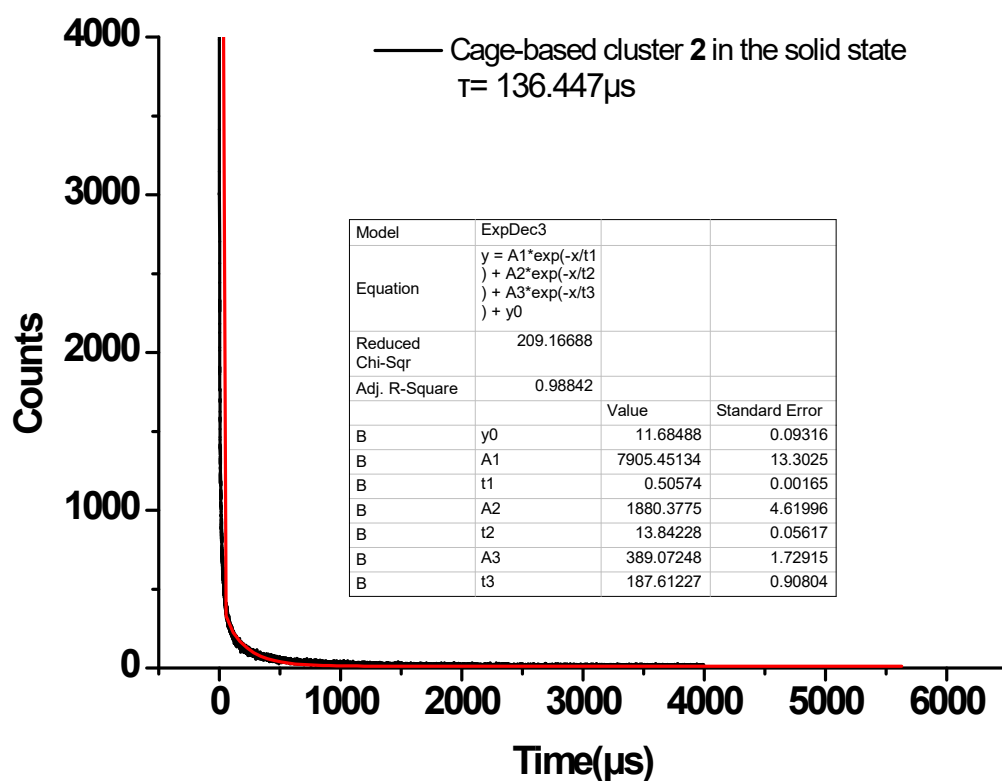
Figure S36. Phosphorescence decay profiles of cluster **2** in the solid state at 298k.
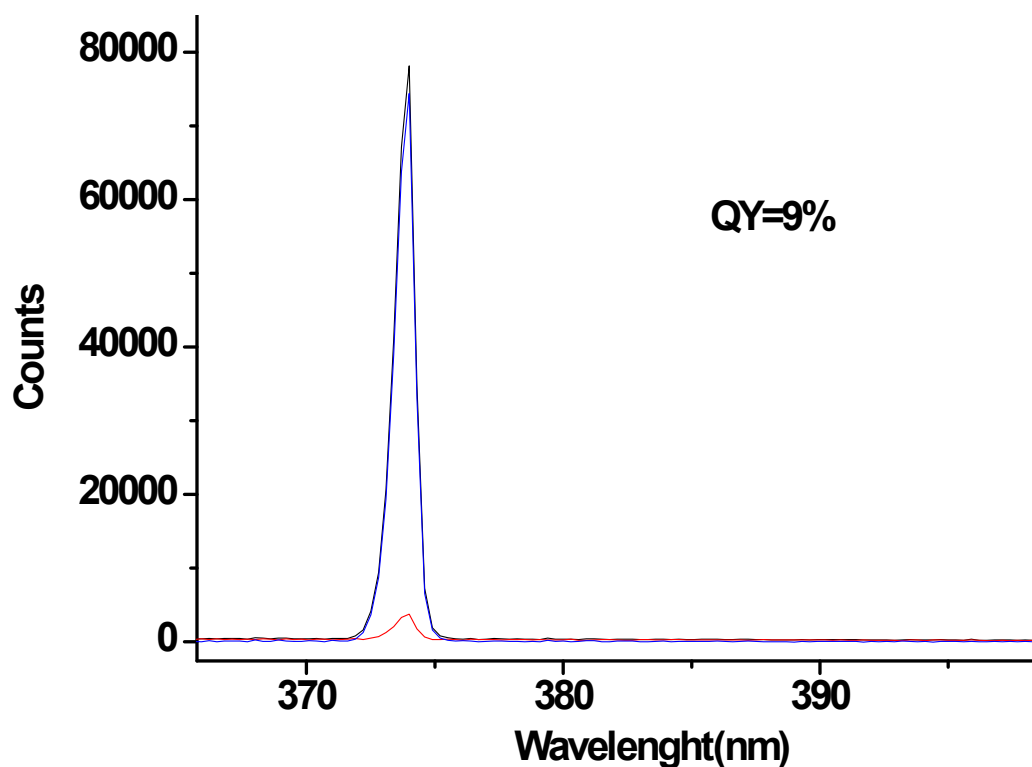
Figure S37. Quantum yield spectra of cluster **2** in the solid state at 298k.

S5. Catalytic 1,3-dipolar cycloaddition of azides with terminal alkynes

S5.1 General procedures for the CuAAC reactions
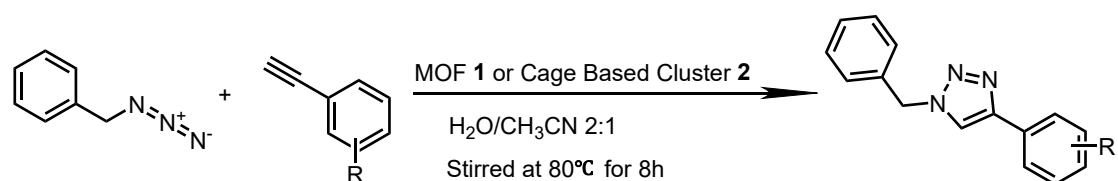
Scheme S4. CuAAC reactions pathway between Benzyl Azide and Phenylacetylene using MOF **1** and Cluster **2** catalyst.

The experimental process of click reaction catalyzed by MOF 1 and cluster 2

A glass assembly tube equipped with a magnetic stir bar was charge with alkyne (0.1 mmol), organic aide (0.11 mmol) and Cu(I) (2.5 mg, 1mol %) in H_2O/CH_3CN (v/v, 2:1, 3mL) under air. The reaction mixture was stirred for about 8h at RT under the WLED. The crude product was purified by column chromatography (eluent: ethyl acetate/petroleum ether = 4:1) to afford white solid. The identity and purity of the

products were verified by ^{1}H NMR and ^{13}C NMR. The results obtained were summarized in Table S5-S6.

Table S5. Summarizes the optimization studies of the CuAAC using MOF **1** or cluster **2** as catalyst[a].

Entry	Catalyst	Solvent	Time (h)	Temperature (℃)/Light	Yield[b] (%)
1	MOF **1**	H_2O	8	rt + WLED	51
2	MOF **1**	CH_3OH	8	rt + WLED	37.6
3	MOF **1**	H_2O/CH_3CN (2:1)	8	80	53
4	MOF **1**	H_2O/CH_3CN (2:1)	8	rt + dark	52
5	MOF **1**	H_2O/CH_3CN (2:1)	8	rt + WLED	75
6	MOF **1**	H_2O/CH_3CN (2:1)	8	80	57
7	MOF **1**	H_2O/CH_3CN (2:1)	8	rt + WLED + 2 eq. TEMPO	45
8	CuI	H_2O/CH_3CN (2:1)	8	rt + dark	31
9	CuI	H_2O/CH_3CN (2:1)	8	rt + WLED	41
10	L[1]	H_2O/CH_3CN (2:1)	8	rt + WLED	NR
11	L[2]	H_2O/CH_3CN (2:1)	8	rt + WLED	NR
12	CuI + L[1]	H_2O/CH_3CN (2:1)	8	rt + WLED	38
13	CuI + L[2]	H_2O/CH_3CN (2:1)	8	rt + WLED	45
14	None	H_2O/CH_3CN (2:1)	8	rt + WLED	NR
15	Cluster **2**	H_2O/CH_3CN (2:1)	8	80	79
16	Cluster **2**	H_2O/CH_3CN (2:1)	8	50	57.4
17	Cluster **2**	CH_3CN	8	rt + WLED	97.8
18	Cluster **2**	Acetone	8	rt+WLED	42
19	Cluster **2**	H_2O/CH_3CN (2:1)	8	rt +WLED	85

| 20 | Cluster **2** | H_2O/CH_3CN (2:1) | 8 | rt +dark | 53 |
| 21 | Cluster **2** | H_2O/CH_3CN (2:1) | 8 | rt + WLED + 2 eq. TEMPO | 30 |

[a] Reaction conditions: Benzyl azide (0.1 mmol), Phenyl alkyne (0.11 mmol), MOF **1** catalyst (1%, 0.001 mmol);

[b] The yield of product isolated was calculated through column chromatography, NMR analysis.
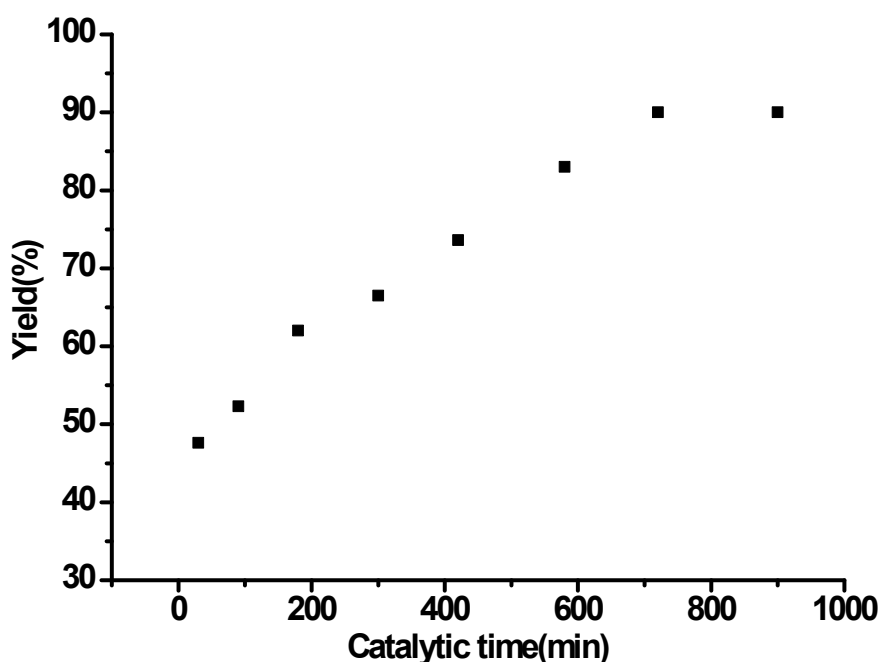
Figure S38. Kinetic study of photocatalytic CuAAC reaction under WLED irradiation using cluster-based cluster **2** as catalyst in H_2O/CH_3CN solution.

S7.2 Recycling of the Cluster 2 catalyst

The cyclability of cluster **2** catalyst is the key to catalytic reaction. Therefore, we attempted to reuse the catalyst cluster **2** after it was removed from the CuAAC reaction. Both catalysts and product can be easily separated from the organic phase by centrifugation, as the "click" product is soluble in the dichloromethane. So catalysts that washed by dichloromethane dried at 80°C for 1h, After changing to another series of substrates, the above catalysts was directly added. After triple cycle was run, the isolated yield did not change significantly, and then the H_2O /CH_3CN(v/v, 2:1, 3mL)

phase was collected.
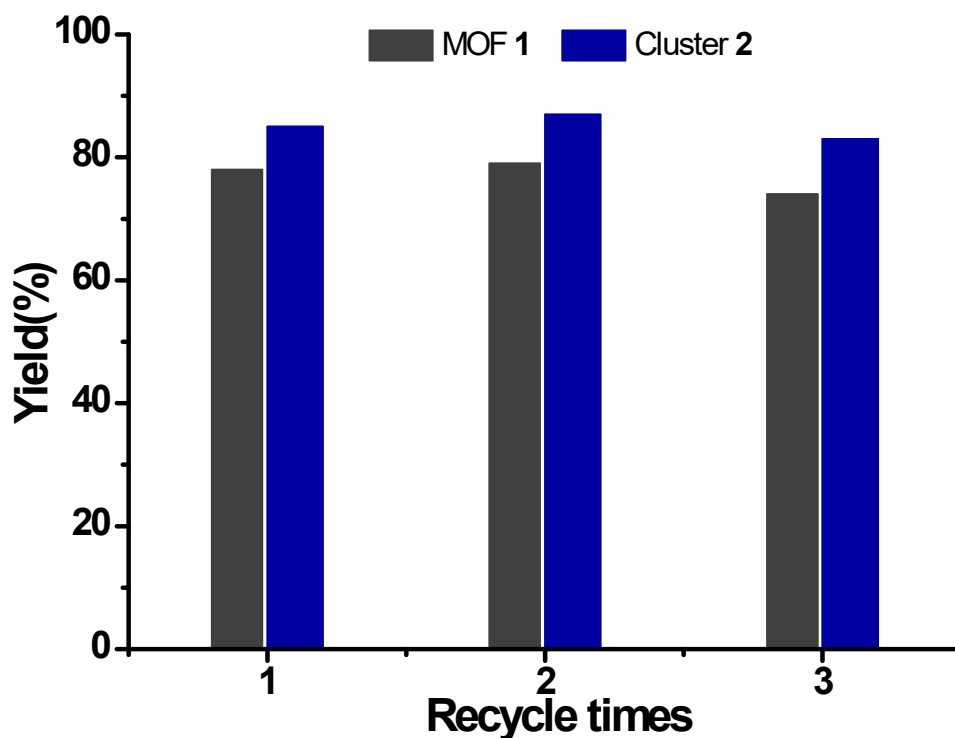
Figure S39. Catalysis yield of MOF **1** and cluster **2** until the third recycling of the catalyst.
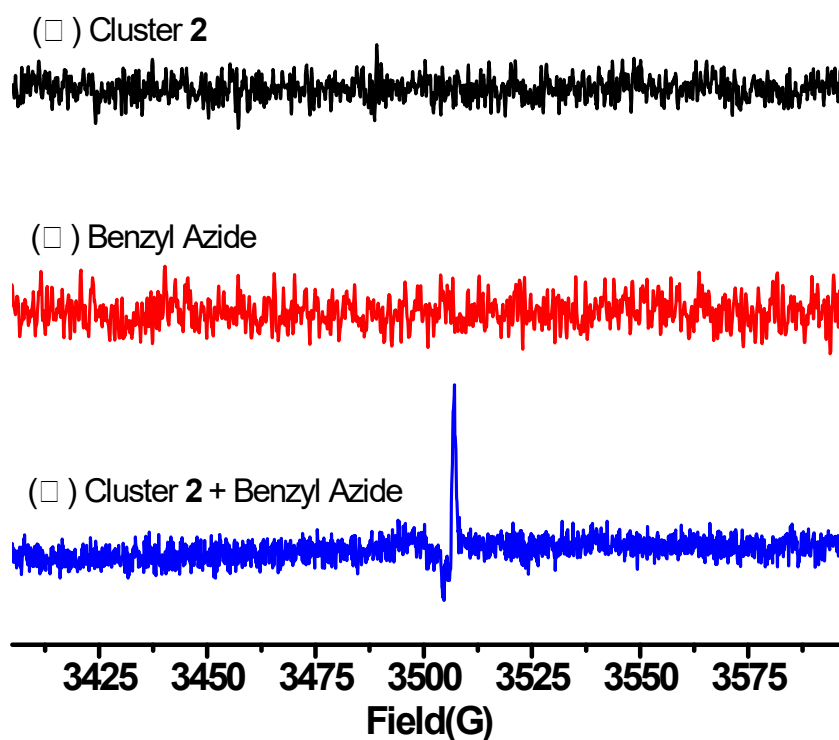
Figure S40. The solution EPR spectrum of cluster **2** and azide under WLED irradiation in CH$_3$CN solution (C = 0.5 mM) at rt for 8h.

S5.2 Characterization of the click products.
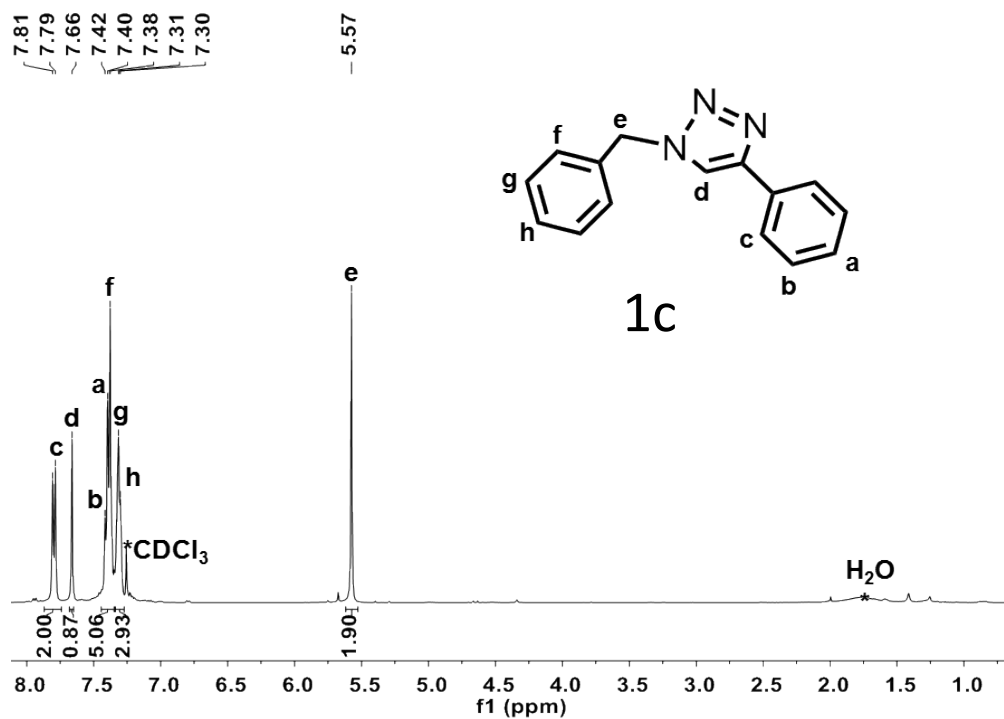
Figure S41. ¹H NMR (400 MHz, CDCl₃) for 1-benzyl-4-phenyl-1H-1,2,3-triazole: δ =7.80 (d, J = 7.4 Hz, 2H), 7.66 (s, 1H), 7.44 – 7.35 (m, 5H), 7.31 (d, J = 5.0 Hz, 3H), 5.57 (s, 2H).
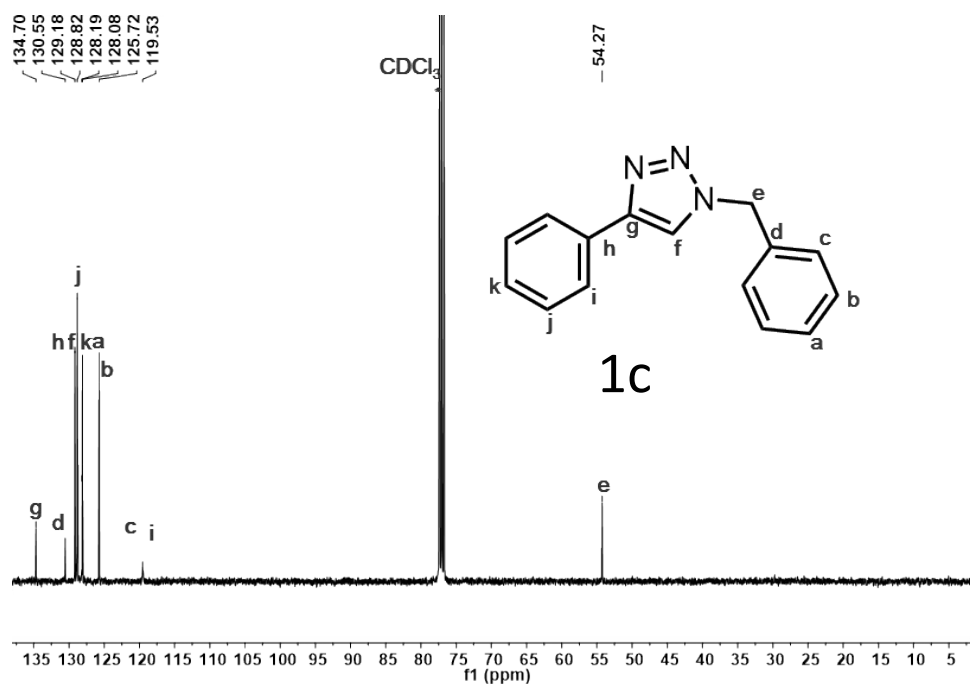
Figure S42. ^{13}C NMR (100 MHz, CDCl$_3$) for 1-benzyl-4-phenyl-1H-1,2,3-triazole: δ =129.18 , 128.82 , 128.19 , 128.08 , 125.72 , 119.53 , 54.27 .
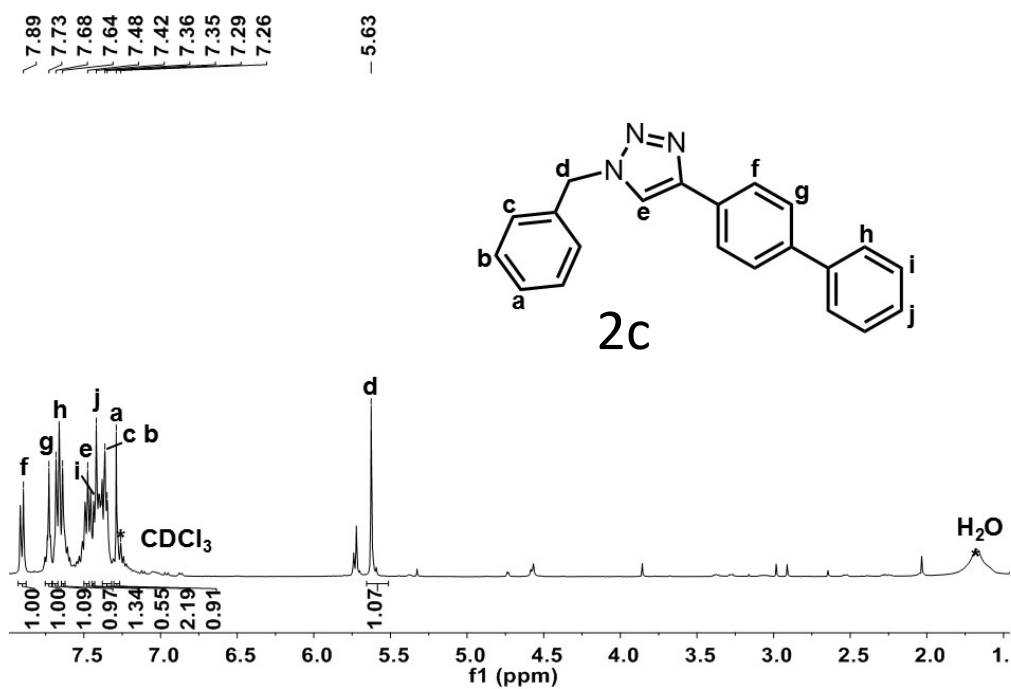
Figure S43.^{1}HNMR(400MHz, CDCl$_3$) for 4-([1,1'-biphenyl]-4-yl)-1-benzyl-1H-1,2,3-

triazole: δ =7.89 (s, 1H), 7.73 (s, 1H), 7.68 (s, 1H), 7.64 (s, 1H), 7.48 (s, 1H), 7.44 (d, J = 1.4 Hz, 1H), 7.36 (d, J = 5.8 Hz, 2H), 7.29 (s, 1H), 5.63 (s, 1H).
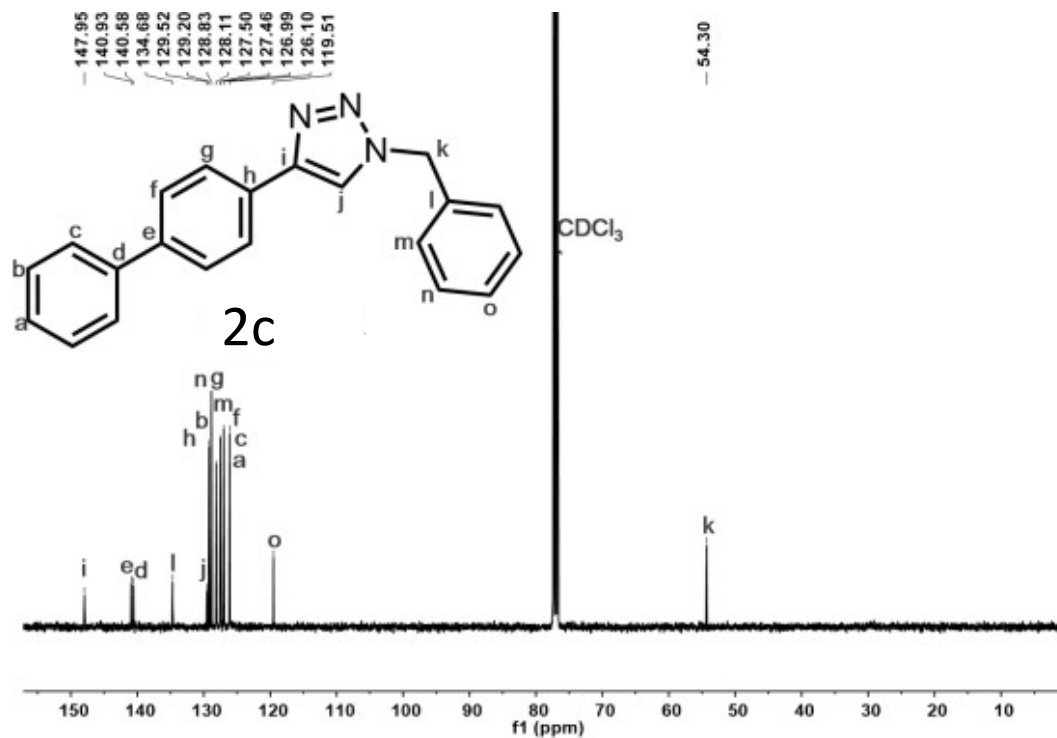
Figure S44. ^{13}C NMR (100 MHz, CDCl$_3$) for 4-([1,1'-biphenyl]-4-yl)-1-benzyl-1H-1,2,3-triazole: δ =147.95, 134.68, 129.52, 129.20, 128.83, 128.11, 127.50, 127.46, 126.99, 126.10, 119.51, 54.30.
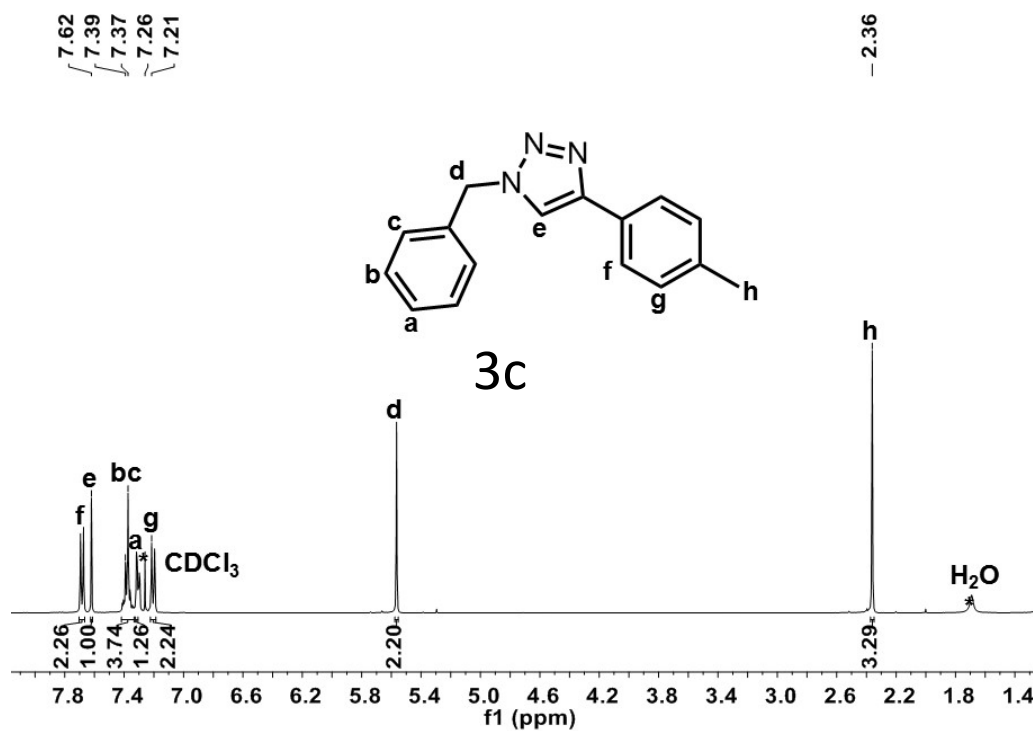
Figure S45. ^{1}H NMR (400 MHz, CDCl$_3$) for 1-benzyl-4-p-tolyl-1H-1,2,3-triazole: δ = 7.70 – 7.67 (m, 2H), 7.62 (s, 1H), 7.38 (d, J = 7.2 Hz, 4H), 7.31 (d, J = 2.4 Hz, 1H), 7.21 (s, 2H), 5.57 (s, 2H), 2.36 (s, 3H).
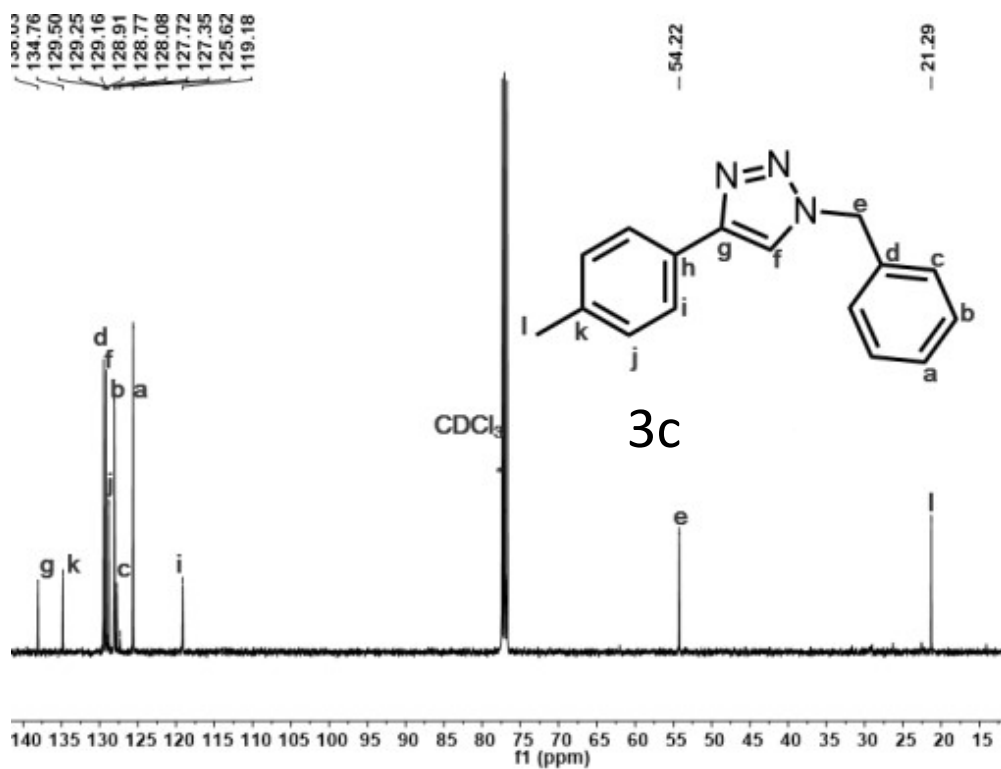
Figure S46. ^{13}C NMR (100 MHz, CDCl$_3$) for 1-benzyl-4-p-tolyl-1H-1,2,3-triazole:

δ=148.33, 138.03, 134.76, 129.50, 129.16, 128.77, 128.08, 127.72, 125.62, 119.18, 54.22, 21.29.
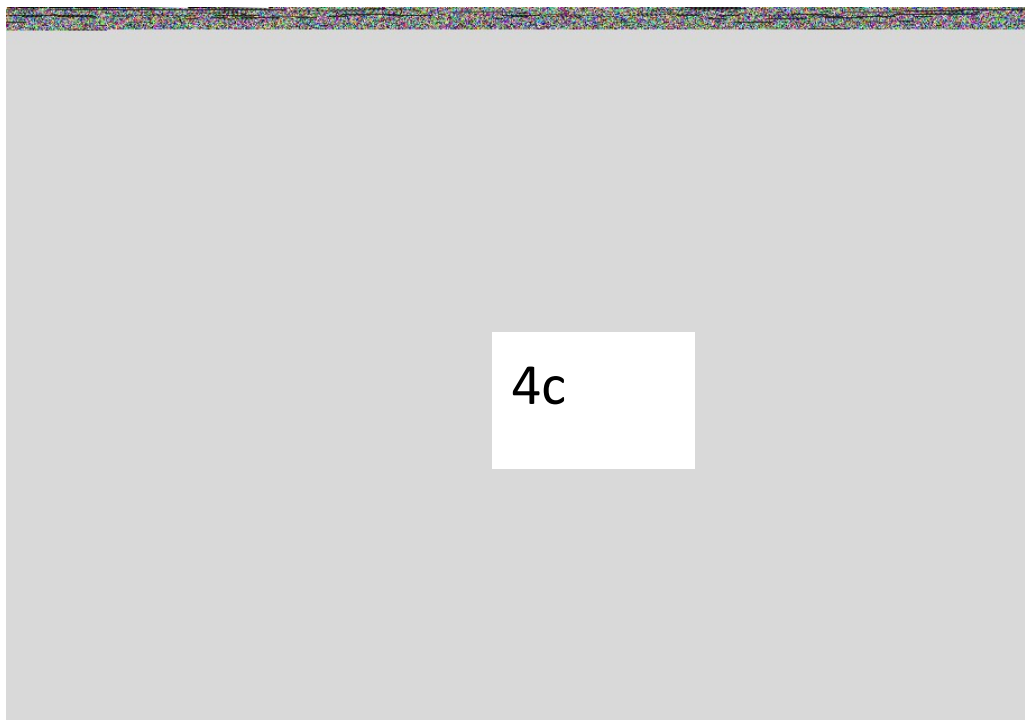
FigureS47. ^{1}H NMR (400 MHz, CDCl$_3$) for 1-benzyl-4-(3-fluorophenyl)-1H-1,2,3-triazole: δ = 7.67 (s, 1H), 7.55 (s, 1H), 7.51 (s, 1H), 7.44 – 7.40 (m, 1H), 7.36 (d, J = 23.8 Hz, 4H), 7.31 (t, J = 2.6 Hz, 1H), 7.00 (s, 1H), 5.58 (s, 2H).
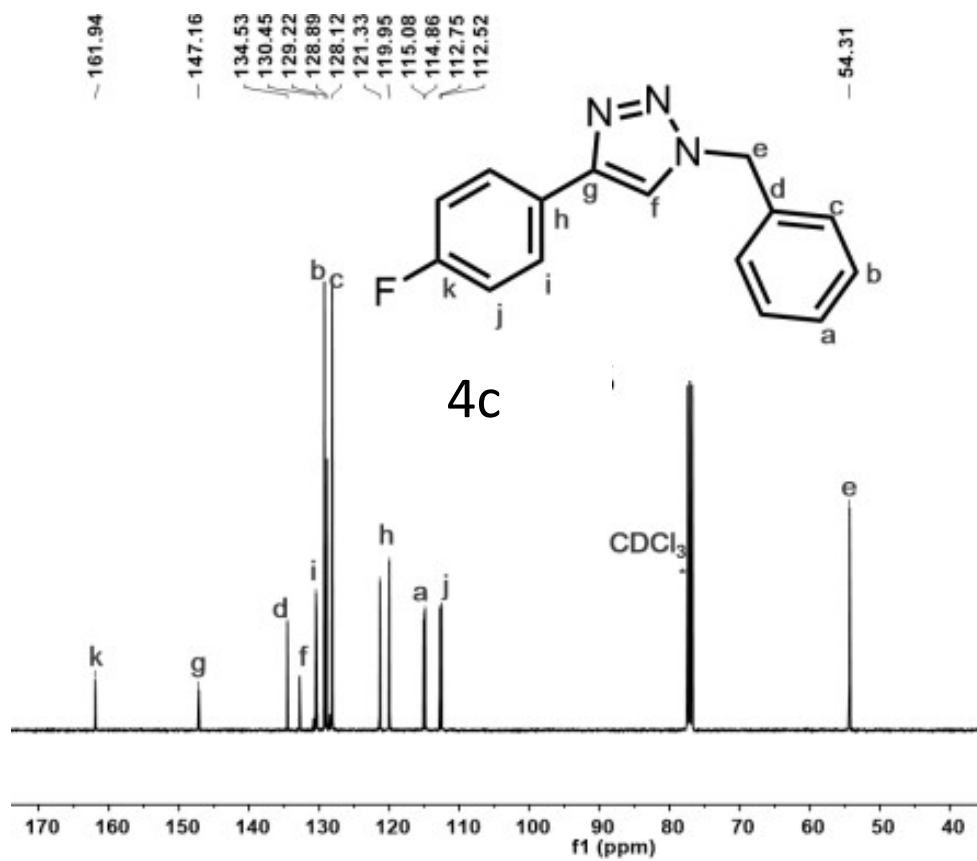
FigureS48.^{13}C NMR (100 MHz, CDCl$_3$) for 1-benzyl-4-(3-fluorophenyl)-1H-1,2,3-triazole: δ =134.53, 130.45, 129.22, 128.89, 128.12, 121.33, 119.95, 115.08, 114.86, 112.75, 112.52, 54.31.
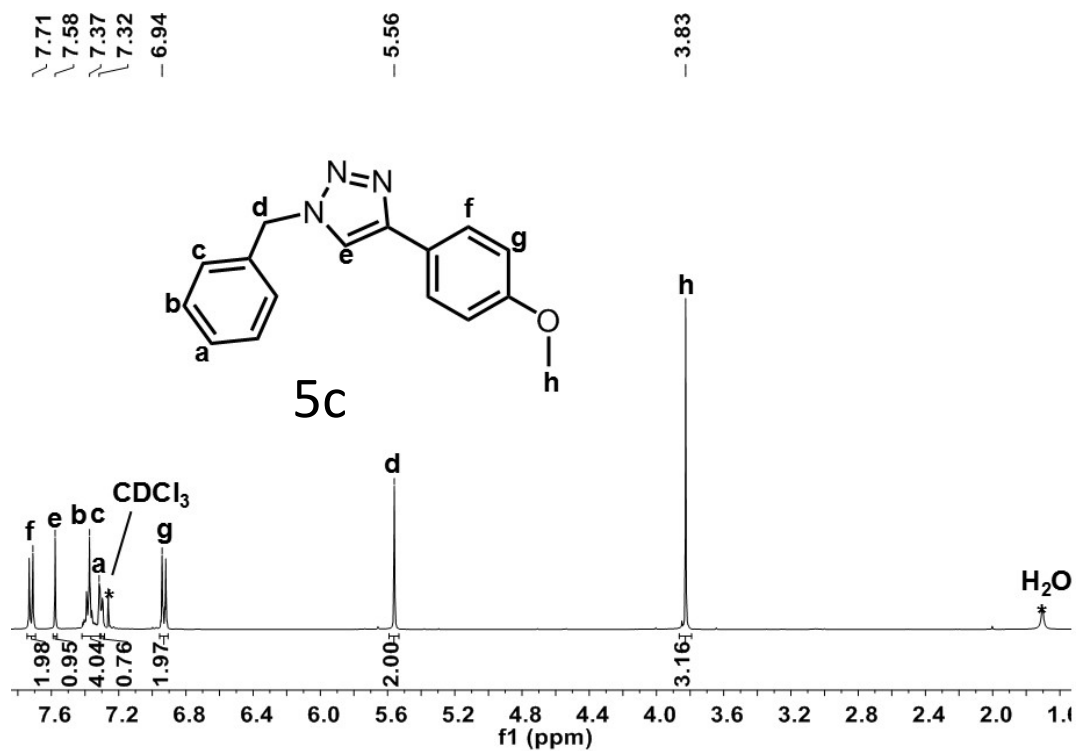
FigureS49. ¹H NMR (400 MHz, CDCl₃) for benzyl-4-(4-methoxyphenyl)-1H-1,2,3-triazole: δ = 7.71 (s, 2H), 7.58 (s, 1H), 7.34 (d, J = 22.8 Hz, 4H), 7.30 (d, J = 1.8 Hz, 1H), 6.94 (s, 2H), 5.56 (s, 2H), 3.83 (s, 3H).
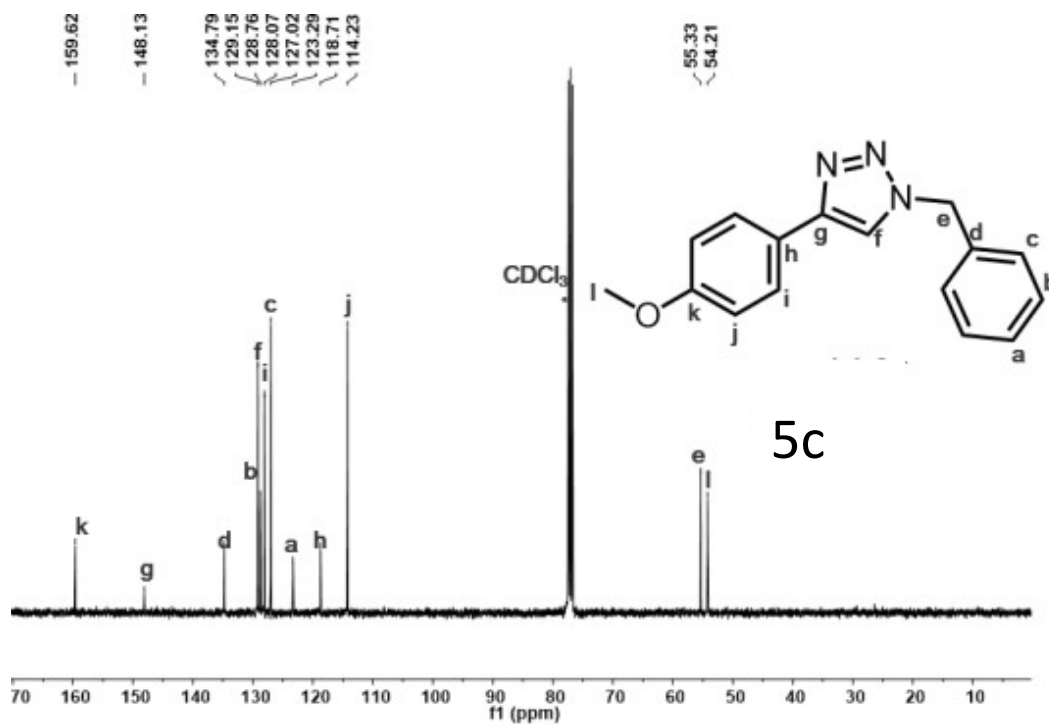
Figure S50. ^{13}C NMR (100 MHz, CDCl$_3$) for benzyl-4-(4-methoxyphenyl)-1H-1,2,3-triazole: δ =159.62, 148.13, 129.15, 128.76, 128.07, 127.02, 123.29, 118.71, 114.23, 55.33, 54.21.
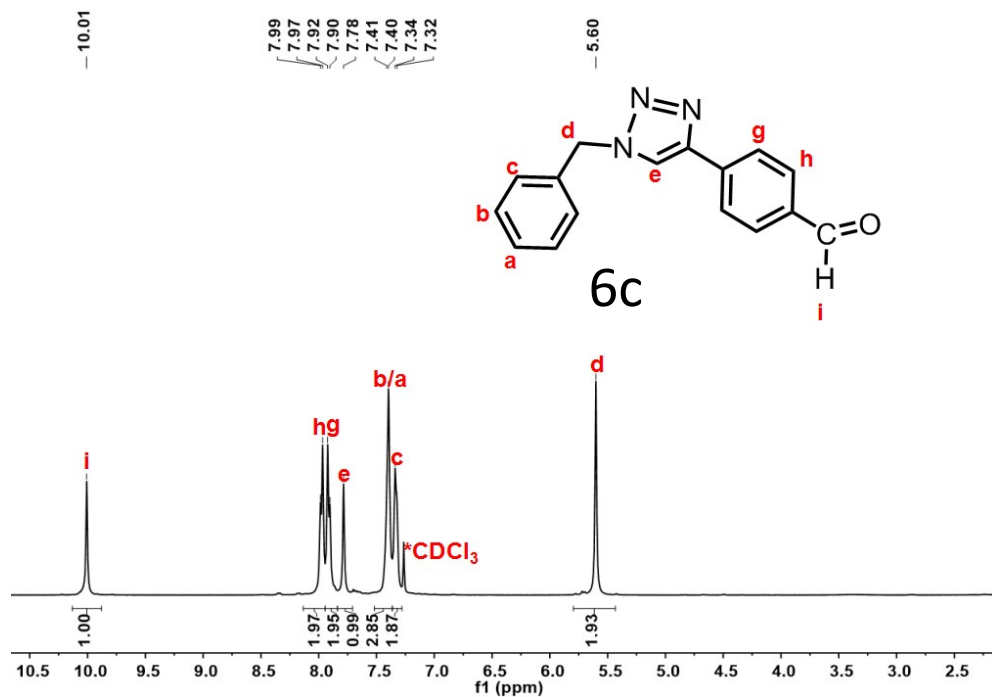
Figure S51. ^1H NMR (400 MHz, CDCl$_3$) for 1-benzyl-4-(3-chlorophenyl)-1H-1,2,3-triazole: δ =10.01 (s, 1H), 7.98 (d, J = 7.9 Hz, 2H), 7.91 (d, J = 8.0 Hz, 2H), 7.78 (s, 1H), 7.40 (d, J = 6.5 Hz, 3H), 7.33 (d, J = 6.7 Hz, 2H), 5.60 (s, 2H).
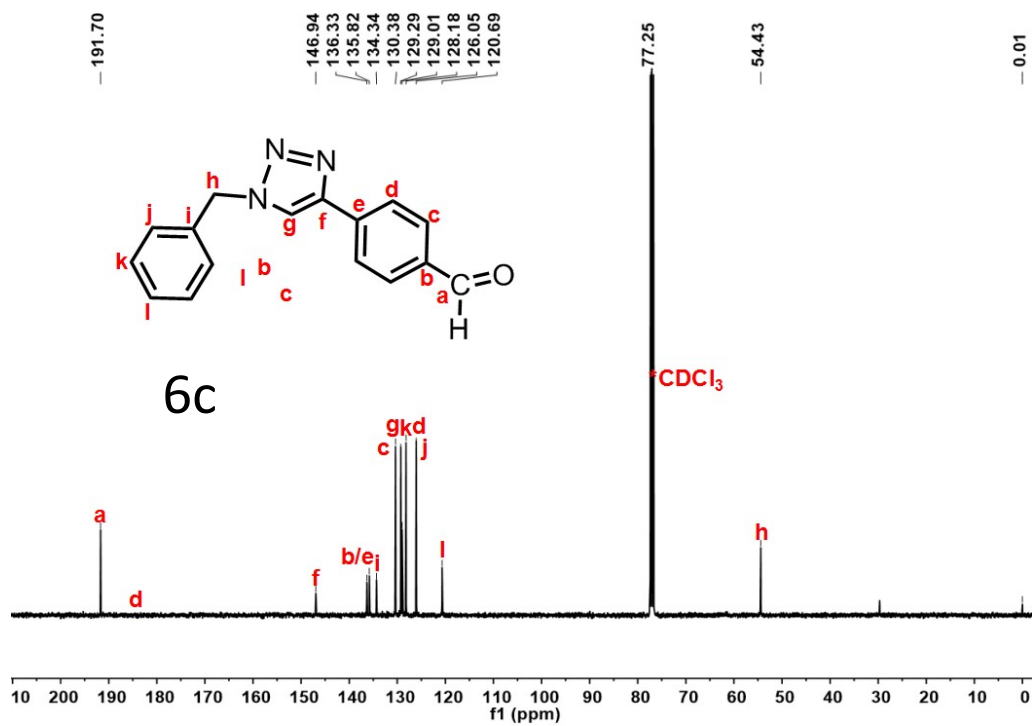
Figure S52. ^{13}C NMR (100 MHz, CDCl$_3$) for 4-(1-benzyl-1H-1,2,3-triazol-4-yl)benzaldehyde: δ=191.70, 146.94, 136.33, 135.82, 134.34, 130.38, 129.29, 129.01, 128.18, 126.05, 120.69, 54.43.
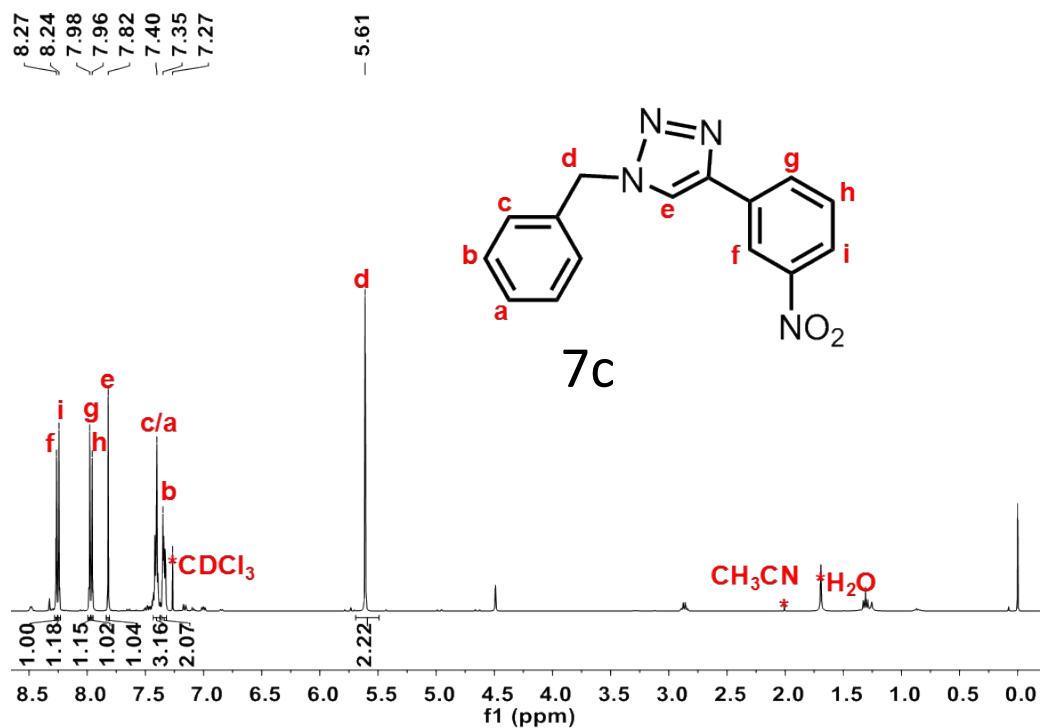
Figure S53. ^{1}H NMR (400 MHz, CDCl$_3$) for 1-benzyl-4-(3-nitrophenyl)-1H-1,2,3-triazole: δ 8.27 (s, 1H), 8.24 (s, 1H), 7.98 (s, 1H), 7.96 (s, 1H), 7.82 (s, 1H), 7.40 (s, 3H), 7.35 (s, 2H), 5.61 (s, 2H).
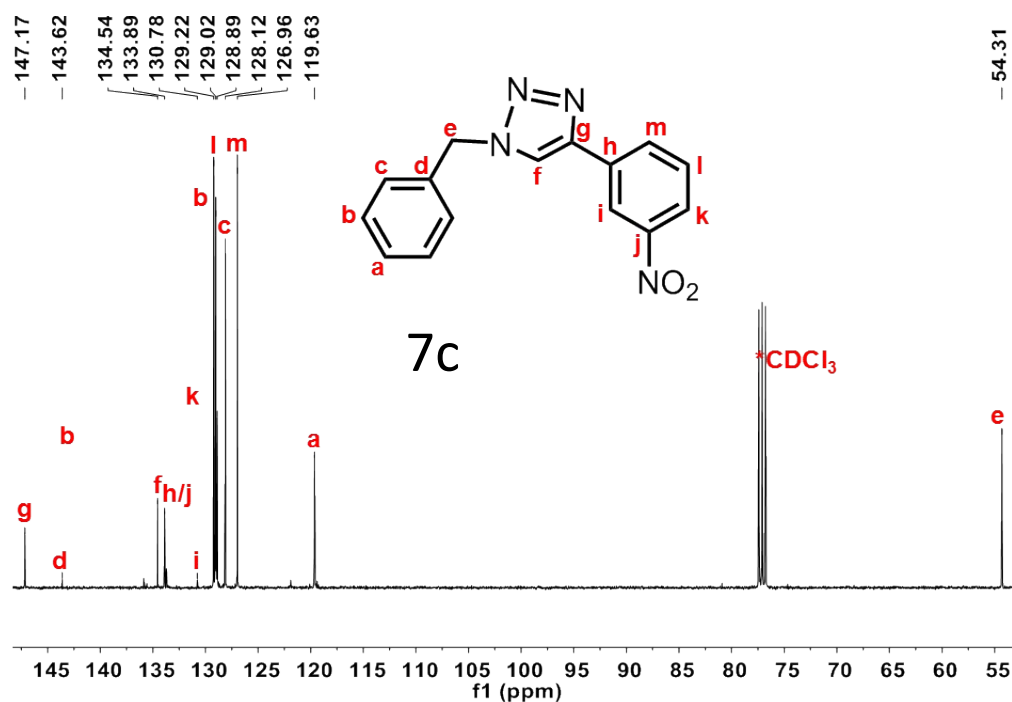
Figure S54. ^{13}C NMR (100 MHz, CDCl$_3$) for triazole-based   compound **3f** (1-benzyl-4-(3-nitrophenyl)-1H-1,2,3-triazole(: δ =13C NMR (101 MHz, Chloroform-d) δ 147.17 , 134.54 , 133.89 , 129.22 , 129.02 , 128.89 , 128.12 , 126.96 , 119.63 , 54.31 .

Reference

[1] Yu-Jing Hu, Jin Yang, Ying-Ying Liu, Shuyan Song, and Jian-Fang Ma.A Family of Capsule-Based Coordination Polymers Constructed from a New Tetrakis (1,2,4-triazol -ylmethyl) resorcin [2]arene Cavitand and Varied Dicarboxylates for Selective Metal-Ion Exchange and Luminescent Properties. Crystal Growth & Design. 2015, 15(8), 3822-3831